DNA methylation profiles in red blood cells of adult hens correlate to their rearing conditions

Fábio Pértille[1, 2], Margrethe Brantsæter[3], Janicke Nordgreen[3], Luiz Lehmann Coutinho[2], Andrew M. Janczak[3], Per Jensen[1] and Carlos Guerrero-Bosagna[1,*]

1-Avian Behavioral Genomics and Physiology Group, IFM Biology, Linköping University, Linköping, Sweden, 58 183.

2- Animal Biotechnology Laboratory, Animal Science and Pastures Department, University of São Paulo (USP)/ Luiz de Queiroz College of Agriculture (ESALQ), Piracicaba, São Paulo, Brazil.

3- Animal Welfare Research Group, Department of Production Animal Clinical Science, Faculty of Veterinary Medicine, Norwegian University of Life Sciences, Oslo, Norway

*Corresponding Author: Email: carbo@ifm.liu.se, Ph +46 13 282321

Abstract-

Stressful conditions are common in the environment where production animals are reared. Stress in animals is usually determined by the levels of stress-related hormones. A big challenge, however, is in determining the history of exposure of an organism to stress, because the release of stress hormones can show an acute (and recent) but not a sustained exposure to stress. Epigenetic tools provide an alternative option to evaluate past exposure to long-term stress. Chickens provide a unique model to study stress effects in the epigenome of red blood cells (RBC), a cell type of easy access and nucleated in birds. The present study investigates in chickens whether two different rearing conditions can be identified by looking at DNA methylation patterns in their RBCs later in life. These conditions are rearing in open aviaries versus in cages, which are likely to differ regarding the amount of stress they generate. Our comparison revealed 115 genomic windows with significant change in RBCs DNA methylation between experimental groups, which were located around 53 genes and within 22 intronic regions. Our results set the ground for future detection of long-term stress in live production animals by measuring DNA methylation in a cell type of easy accessibility.

Keywords: Red blood cells, epigenetics, chicken, DNA methylation, animal welfare, rearing

Introduction-

Stress in production animals generated by unsustainable production methods is a frequent issue of concern. Besides the ethical issue of inducing unnecessary stress in animals, detrimental practices in the animal production industry have consequences from a human health perspective (Rostagno, 2009). The environment where production animals are reared influences not only their later health and wellbeing but also the quality of the food originating from them (Broom, 2010). Stressful conditions to which production animals can be subjected include extreme illumination patterns (Morgan and Tromborg, 2006; Olanrewaju et al., 2006), social isolation or crowding (Goerlich et al., 2012), food restriction (Morgan and Tromborg, 2006; Savory and Lariviere, 2000), too high or too low temperatures, restriction of movement, barren environments, and lack of appropriate substrates for foraging, exploration and manipulation (Morgan and Tromborg, 2006).

Stress in animals is associated with a cascade of hormonal responses (Henry, 1992). The primary physiological stress response observed is an increase in the hypothalamic-pituitary-adrenal (HPA) axis activity, which results in elevated levels of the glucocorticoids (Fallahsharoudi et al., 2015). Initially, increases in testosterone levels related to increased anxiety are observed (Henry, 1992). Subsequently, decreases in the noradrenaline/adrenaline ratio are observed, concomitant with increases in adrenaline, prolactin and fatty acids (Henry, 1992). In conditions of further distress, adrenocorticotropic hormone and cortisol levels will increase (Henry, 1992). Due to this plethora of hormonal changes generated by stressful conditions, stress in animals is usually determined by the levels of stress-related hormones such as cortisol and adrenaline (Ishibashi et al., 2013; Muller et al., 2013). A big challenge, however, is in determining the history of the exposure of an organism to stress, given that the release of stress hormones can show an acute (and recent) but not a sustained exposure to stressful conditions (Henry, 1992).

An alternative option to the use of hormonal measurements to evaluate past exposure to long-term stress could be to utilize epigenetic tools instead. Epigenetics involves studying how environmental exposures affect gene regulation during the lifetime of organisms. Epigenetic changes are defined as

accessory chemical modifications of the DNA that regulate gene expression and are mitotically stable (Skinner et al., 2010). These modifications include DNA methylation or hydroxymethylation of nucleotides, chemical modifications of histones, interaction of DNA with small RNAs, or states of chromatin condensation (Denham et al., 2014; Feil and Fraga, 2011; Teperek-Tkacz et al., 2011). Altering epigenetic states can lead to distinguishable phenotypic consequences such as changes in the coat color (Dolinoy et al., 2007) or increased propensity to diseases (Guerrero-Bosagna and Skinner, 2012). A variety of organism models has been used in epigenetic research, including laboratory rodents (Dolinoy et al., 2007; Guerrero-Bosagna et al., 2008; Susiarjo et al., 2013), flies (Seong et al., 2011), honey bees (Dickman et al., 2013; Lyko et al., 2010), plants (Cubas et al., 1999; Manning et al., 2006) and yeast (Zhang et al., 2013). However, in spite of the importance of epigenetic mechanisms in biology in general, epigenetic studies in production animals are scarce. Among production animals, chickens have been suggested as a promising model for epigenetic studies (Fresard et al., 2013). Two important reasons for this are that chickens have had their genome extensively sequenced (Rubin et al., 2010) and have historically been an important model for translational research with implications for human health and physiology (Kain et al., 2014).

Long term stress is known to generate life-long changes in stress susceptibility that is correlated to epigenetic changes (Jensen, 2014). Thus, it is expected that if animals are constantly subjected to stress and systemic hormonal changes, this exposure will imprint the epigenome of blood cells. Epigenetic changes in blood cells will then serve as markers of past exposure to stress. Research in humans (Malan-Muller et al., 2014) and monkeys (Provencal et al., 2012) have shown that stress affects DNA methylation in blood cells. The epigenome of blood cells can provide a meaningful assessment of biological processes involved in stress because disruptions of the HPA-axis have systemic consequences (Zannas and West, 2014). Since different practices in the production environment will generate different levels of stress in animals, it is practical (from the perspective of evaluation of long term stress) to understand how stress correlates with specific epigenetic profiles in production animals. Chickens provide an excellent model to study epigenetic profiles of long-term stress, since they represent the second most consumed meat source worldwide (behind pig meat)

(OECD-FAO, 2015) and because avian species, unlike mammals, contain nucleated red blood cells (RBCs). This allows for accurate epigenetic profiling because RBCs are a cell type simple to purify that can be obtained from live animals.

The present study aims at investigating in chickens whether two different rearing conditions can be identified by looking at epigenetic patterns in their RBCs later in life. The conditions tested are rearing in a system of open aviaries versus rearing in cages. These two different rearing conditions are likely to differ with regards to the amount of stress the birds are exposed to. When tested at 19 and 23 weeks of age, the aviary-reared birds moved more and spent more time close to a human and a novel object compared with the cage-reared birds (Brantsaeter et al., 2016). These results are indicative of aviary-rearing reducing the birds' underlying fearfulness. Additionally, cage-rearing was found to reduce the birds' short-term memory two months after transfer from the rearing farm compared to aviary-reared birds, when assessed in a hole-board memory test (Tahamtani et al., 2015). The objective of using this model is to generate a proof-of-concept for future detection of long-term stress in production animals using epigenetic measurements in cell types of easy accessibility in live animals. The identification of a correlation between RBCs epigenetic profiles and long-term stress will overcome limitations that exist when evaluating stress through hormonal levels or visual health assessments, which do not provide reliable accounts of long-term stress.

In order to identify DNA methylation profiles related to different rearing conditions in chickens, we compared RBCs DNA methylation in a group of birds reared in cages (a common housing system, with low environmental complexity) with that of birds reared in open aviaries (which represents a complex environment). Previous studies have shown that chickens reared in a complex aviary system are less fearful, use elevated areas of the pen more often as adults (Brantsaeter et al., 2016), and have better spatial working memory (Tahamtani et al., 2015) than laying hens reared in a simpler cage environment. The present study tests whether the different rearing conditions applied, which associate with different levels of environmental complexity, stimulation of cognitive capabilities and responses to stress, will have long term effects in the blood methylome of chickens. Our comparison revealed

115 genomic windows with significant change in RBCs DNA methylation between experimental groups, which were located within or in the vicinity of 53 genes and within 22 intronic regions. Our results set the ground for future detection of long-term stress in live production animals by measuring DNA methylation in a cell type of easy accessibility. The present results can be used as a proof-of-concept for the future identification of epigenetic marks (signatures) related to past stress conditions that occur in the production environment.

Materials and methods-

Ethical statement

All experimental protocols employed in the present study that relate to animal experimentation were approved by the Institutional Animal Care and Use Committee at the Norwegian University of Life Sciences under the resolution ID number 6190, in order to ensure compliance with international guidelines and regulations for the ethical use of animals in scientific research.

Subjects and rearing treatments

The study was conducted using non beak-trimmed, female Dekalb white chickens (*Gallus gallus domesticus*), aged 0–23 weeks with normal health status. Birds were hatched at a commercial hatchery and immediately brought to a rearing farm. All birds were housed within the same room. Initially, all birds were kept confined inside the aviary row, with access to food and water. When the birds were four weeks of age, access to the aviary corridors was given to half of them, as this is the normal procedure in aviary rearing systems. This group was named “aviary reared-birds” (AV). The other half of the birds was kept under confinement in the aviary row for the entire rearing period. The group of birds staying inside the cages was named “cage-reared birds” (CA). These two rearing conditions were maintained until the birds were 16 weeks of age. After the rearing period had ended, a random subset of birds from each treatment was moved to the experimental facilities for blood sampling, which occurred at 24 weeks of age. A schematic representation of the experimental design is shown in Figure 1A.

Rearing system conditions

The housing system in the single room in which all birds were housed was Natura Primus 1600 (Big Dutchman; http://www.bigdutchmanusa.com) designed for aviary-rearing of laying hen pullets. This system consisted of cages stacked in three tiers placed on either side of a corridor for allowing inspection by the caretaker. Cage dimensions were 120 cm × 80 cm × 60 cm (length × width × height). Each aviary cage contained a 120 cm feed trough, one 120 cm perch, and five drinking nipples. All the cages could be opened at the front, allowing the birds to move freely between each tier and the floor of the corridor. Ramps run from the floor to the second tier to increase ease of access for pullets. When cage doors are in the open position, perches extend from the front of the first and second tiers. The density was 25 birds/m^2 for both treatments during the first four weeks of life. Chick paper covered 30% of the wire mesh floor of the cages in sufficient amounts to last until the birds were released out in the corridors.

During rearing, all birds were exposed to the same light intensity, light schedule, and temperatures, as recommended by the General Management Guide for Dekalb White Commercial Layer (Hendrix, 2015). They were provided with ad libitum access to feed using a chain dispersal system and ad libitum access to water. The feed type was conventional pullet feed produced and sold by Felleskjøpet, Norway ("Kromat oppdrett 1" for 0- to 6-week-old birds, "Kromat avl egg 1" for 6- to 8-week-old birds, and "Kromat oppdrett 2" for 8- to 15-week-old birds).

Blood collection and DNA extraction

Blood samples were collected from 21 individuals (9 AV and 12 CA) of 24 weeks of age. Before blood sampling chickens were sedated using 0.5 ml/Kg Zoletil mix, which contains 10 ml Rompun (Xylazine 20 mg/ml) and 0.75 ml Butomidor (Butorphanol 10 mg/ml) mixed with Zoletil powder (Tiletamine HCL 125 mg and Zolazepam HCL 125 mg). Blood samples were collected as soon as the birds were considered unconscious, which occurred within a maximum timeframe of 10 minutes. Birds were then humanely euthanized by cervical dislocation. Each blood sample was collected using a 1 ml syringe and a BD Microlance cannula (21G x ½", 0.80 x 40 mm). A total of 160 µg of blood

was then transferred from each sample into two heparinized glass capillaries, which were then centrifuged at 3000 RPM for 5 minutes. After centrifugation, the tubes were manually broken into two pieces, one of them containing the hematocrit fraction, which was placed inside 1.5 mL micro-centrifuge tubes and stored in a -80°C freezer until further analyses.

DNA extraction was performed through proteinase K digestion. Initially 10 µL of the hematocrit fractions were incubated with 200 µl of extraction buffer (1M Tris-HCL, 0.5 M EDTA, 10% SDS) and 20 µL of 0.1 M DTT at 65°C for 15 min. Then, incubation with 20 µL of proteinase K (20mg/mL) was performed overnight at 55°C under rotation. After proteinase K digestion samples were incubated with Protein Precipitation Solution (Promega) for 15 min on ice and centrifuged for 20 min at 13000 rpm and 4°C in a benchtop microcentrifuge. The supernatants (1 mL) were transferred to new tubes and DNA was precipitated with equal amounts of 100% isopropanol. In addition, 3 µL of glycogen (5 mg/mL) was added to improve further visualization of DNA pellets. After 30 min of incubation at 4°C the samples were centrifuged at 13000 rpm and 4°C for 30 min. The supernatants were discarded and the DNA pellets were washed with ice cold 70% ethanol, followed by centrifugation at 13000 rpm and 4°C for 10 min. The supernatants were discarded again and the pellets in the tubes were dried out in a heating block at 55°C for 5 min. DNA pellets were re-suspended in 200 uL of ultrapure water.

DNA methylation analyses

In order to perform DNA methylation analyses in a cost effective manner, we have combined a Genotyping by Sequencing method (Pértille et al., 2016) with the technique of Methylated DNA immunoprecipitation (Guerrero-Bosagna and Jensen, 2015). We have recently described the optimization of each of these two methodologies separately for its use with chicken DNA (Guerrero-Bosagna and Jensen, 2015; Pértille et al., 2016). This combination of methods was needed because current methods that assess DNA methylation in reduced genomes perform such a reduction through enzymatic digestion targeting restriction sites that contain CpG sites (Gu et al., 2011). Moreover, such

an approach is highly biased towards CpG islands (Gu et al., 2011). Our approach, instead, reduces the genome by digesting on restriction sites unrelated to CpGs and is unbiased towards CpG islands.

We first digested the genome with *PstI* (Thermo Scientific) as previously described (Pértille et al., 2016). After this fragmentation had generated a significantly reduced genome (approximately 2% of its original size) and enrichment of small fragments in a suitable range for Illumina sequencing (200-500 bp) (Pértille et al., 2016), the methylated fraction was captured by an anti-methyl-cytosine antibody (Diagenode, catalog number C15200006, 2 µg/µL) as previously described (Guerrero-Bosagna and Jensen, 2015). The output of the methylated DNA immunoprecipitation (MeDIP) was used as the input of GBS. The GBS method uses ligation steps in which a barcode adapter (identifying individual samples) and a common adapter for Illumina sequencing barcoding system are ligated at each end of the digested DNA fragments (Poland and Rife, 2012). Due to the barcoding system, the GBS technique enables the creation of a sequencing library with DNA pooled from several individuals (Elshire et al., 2011; Poland and Rife, 2012). Once the barcodes and adaptors are ligated, PCR is performed followed by clean-up of primer dimers and unbound adapters (Elshire et al., 2011; Poland and Rife, 2012). A detailed description of the method for its use in chickens has been previously reported (Pértille et al., 2016). The use of the present approach, in which these two methodologies are combined, allowed us to scan the RBCs methylome of 21 chickens using only half of an Illumina sequencing lane. Sequencing was performed paired-end with read length of 125 bp on the Illumina HiSeq2500 platform, at the SNP&SEQ facilities of the SciLifeLab (Sweden). The dataset supporting the conclusions of this article is available at the European Nucleotide Archive (ENA) repository (EMBL-EBI), under accession PRJEB13188 (http://www.ebi.ac.uk/ena/data/view/PRJEB21356).

Bioinformatic analyses

SNP call was performed using the Tassel v.3.0 program (Glaubitz et al., 2014) following the default TASSEL-GBS Discovery Pipeline. The alignment of quality-trimmed reads was performed using Bowtie2 tool v.2.2.5 (Langmead and Salzberg, 2012) against the

chicken reference sequence (*Gallus_gallus* 4.0, NCBI). The filtering parameters used were 5% for minimum minor allele frequency (mnMAF), and 50% for minimum site coverage (mnScov) .

For the methylated DNA sequencing, data quality trimming was performed in paired-end short reads with the SeqyClean tool v. 1.9.10 (Zhbannikov et al., 2013) using a Phred quality score ≥24 and a fragment size ≥50. The quality of the reads was checked before and after the cleaning by FastQC v.0.11.3 (Andrew, 2010). The Stacks v.1.39 program was used for data de-multiplexing (Catchen et al., 2011) of quality-trimmed reads. In this procedure, each read stored in a FASTQ file has a identification map key file, a barcode containing matching information for the respective sample. The expected reads begin with one of the individual barcodes and are followed by the cut site remnant for *PstI*, which contains the sequence CTGCA. Fragments are then grouped into individual files, which correspond to individuals identified by their respective barcodes. The option "very sensitive-local alignment" was used in the Bowtie2 tool v.2.2.5 (Langmead and Salzberg, 2012) for the alignment of quality-trimmed reads against the chicken reference sequence *Gallus_gallus* 4.0 (NCBI). Default parameters for paired- and single-end sequences were used. The coverage depth of each sample was checked using Samtools v.0.1.19 (Li et al., 2009) with the "depth" option.

Because low methylated DNA material is obtained after MeDIP of the *PstI*-reduced genome, some samples will contribute with very low DNA amounts to be sequenced. These individuals will show low total number of reads distributed in a few genomic regions, generating a skewed distribution of methylated sites along the genome. This will result in an overestimation of the coverage values in those CpG sites that happened to be covered by reads. To prevent this, we defined a minimum cut-off index in order to select high quality sequenced samples for further testing of differences between experimental groups. This cut-off index was defined by dividing the 'percentage of the Chicken Genome covered' (%Cov) by the 'sequencing coverage average for each sample' (S.Cov) and multiplying by 100 (i.e., cut-off index = %Cov/S.Cov * 100). It was needed to combine the information provided by each of these variables into one single index because 'average individual coverage' *per se* could not be used as the sole criteria due to the fact that some samples have high coverage but only in small factions of the genome. The value of 1.0 was defined as a minimum

threshold, which signifies that at least 1 % of the genome is well covered in that specific sample. Since previous analyses of the chicken genome by GBS alone showed good coverage of ~ 2 % of the genome (Pértille et al., 2016), it is reasonable to expect that less than this value will be well covered when using GBS in combination with MeDIP. By plotting S.Cov vs %Cov we obtained an exponential relationship (Figure S1) in which it can be observed that having a cut-off index of 1 effectively eliminates samples with low %Cov and/or low S.Cov. Based on this, individuals showing cut-off index below 1.0 were discarded from further analyses.

Following read alignment, all analyzes were performed using bioinformatics packages from the "R" Bioconductor repository. The BSgenome.Ggallus.UCSC.galGal4 package was uploaded as the reference genome. The MEDIPS R-package was used for basic data processing, quality controls, normalization, and identification of differential coverage. In order to avoid possible artefacts caused by PCR amplification, MEDIPS allows a maximum number of stacked reads per genomic position. This is done by using a Poisson distribution of stacked reads genome-wide. The default parameter of p=0.001 was used as threshold for the detection of stacked reads. The reads that passed this quality control are then standardized to 100 bp by extending smaller reads to this length, which is the paired-end read size generated by the Illumina HiSeq platform. The genome was divided into adjacent windows of 300 bp length, which is the average length of expected contigs generated by our GBS approach, as well as the program default. MeDIP-seq data is transformed into genome wide relative methylation scores by a CpG dependent normalization method (Chavez et al., 2010). This normalization is based on the dependency between short read coverage and CpG density at genome-wide windows (Down et al., 2008) and can be visualized as a calibration plot. A calibration plot was generated using one of the 10 individuals that passed the cut-off index to generate a coupling set (object that groups information about CpG density genome-wide). Based on this, a threshold for a minimum sum of counts across all samples per window is defined (minRowSum = 10). Sequencing data for each individual is then assigned to one of the experimental groups (AV or CA) and differential coverage (i.e. differential methylation) is calculated between the two conditions. Adjacent windows showing significant change were then merged to generate the DMR obtained. For this, the default value of 1 was used within the function MEDIPS.mergeFrames, allowing to merge the

neighboring significant windows with a 1 base par gap between them. The merged windows were annotated against the chicken reference genome (Gallus_gallus 4.0, NCBI) using the Variant Effect Predictor (VEP) tool (McLaren et al., 2010). The edgeR and heatmap.2 packages (and extensions) were used for the confection of plots.

The internet-based tool Consensus PathDB (Kamburov et al., 2013) (http://cpdb.molgen.mpg.de) was used to perform an analysis of biological pathways enriched by the genes with differentially methylated regions found in our study, as well as gene ontology analyses of these genes. Consensus PathDB (Kamburov et al., 2013) integrates interaction networks based on published information in humans. These interaction networks include complex protein-protein, genetic, metabolic, signaling, gene regulatory and drug-target interactions, as well as biochemical pathways (Kamburov et al., 2013). Another internet-based tool used in this study to identify over -represented pathways related to our gene list was Reactome (Croft et al., 2011), which is an open source curated bioinformatics database of human pathways and reactions (http://www.reactome.org). The advantage of Consensus PathDB over Reactome is that it is capable of accessing a variety of databases that contain previously described biological pathways (e.g., Kegg, Biocarta, Reactome, Wikipathways). However, in order to use Consensus PathDB the genes in the chicken genome had to be extrapolated to humans, since it does not accept the ENSEMBL chicken genome annotation. Therefore Reactome, which did accept the input of chicken genes with the ENSEMBL identifier, was also used. These two tools therefore provided complementary information about our gene list.

Results-

The present experiment compared the RBCs methylome of chickens reared in open aviaries versus in cages, to detect whether epigenetic profiles in RBCs could be identified as correlating to each of these rearing conditions. The experimental procedures are summarized in Figure 1B. RBCs of 21 chickens were extracted in total, being 9 reared in open aviaries and 12 reared in cages. A combination of the Genotype by Sequencing (GBS) and MeDIP methods was used to identify genome-wide changes in DNA methylation.

After sequencing of the reduced-methylated DNA fraction from RBCs of these animals, bioinformatic analyzes were performed and filter parameters were applied. Our quality control procedure selected sequencing data from 4 AV and 6 CA animals for further statistical analyses. In order to account for potential genetic effects generated by the treatments we tested whether fixed allelic differences could be identified between the experimental groups. A total of 248,170 unique sequence tags were obtained from the 21 individuals submitted to the Tassel pipeline, and 83.1% were aligned against the chicken reference genome (Gallus_gallus 4.0, NCBI). A total of 21,093 SNPs were identified across the 10 individuals (4 AV and 6 CG) that passed the cut-off index. Among these SNPS identified, we did not observe any fixed allelic differences between the CA and AV groups, which could have stochastically appeared due to the separation of animals in two groups, or emerged due to the treatment itself.

For the DNA methylation analysis, our method interrogated changes in 810,186 CpG sites per individual, which corresponds to ~7.6% of all CpGs in the chicken genome. An MA plot showing the log-fold change of AV/CA counts per 300 bp genomic windows, which represents changes in DNA methylation, against the normalized window counts is shown in Figure 2A. Genomic windows with significant changes in DNA methylation between groups ($P < 0.0005$) are depicted in red dots. A principal components analysis (PCA) performed using the windows with significant differences in counts ($P < 0.0005$) between the AV and CA groups confirmed that all individuals in the analysis match the initial experimental group separation (Figure 2B). Our comparison revealed that 115 windows showed significant change in DNA methylation between experimental groups (Supplementary Table 1). A heat map showing the windows with significant changes is shown in Figure 3. Adjacent windows showing differential coverage were merged into differentially methylated regions (DMR) between the experimental groups (see Materials and Methods for detailed information), which were located within or in the vicinity (5 kb up- or downstream from the DMR, based on default criteria in the VEP tool) of 53 genes and within 22 intronic regions. Supplementary Table 2 describes the chromosomal location of all DMR, the number of CpGs within them, their annotation, as well as their location within or in the vicinity of genes. Figure 4 summarizes the location of these regions relative to genes (Figure 4A), as well as their chromosomal location (Figure

4B). The fold changes in DNA methylation of the DMR and the direction of these, e.g. hyper- or hypo-methylation of CA reared versus AV, are shown in Figure 5.

A network analysis was performed with the DMR associated genes in Consensus PathDB, which connects biological pathways and gene ontology information (Supplementary Table 3). A simplified pathway showing hypothetical effects of the DMR affected by the treatment is shown in Figure S2.A (redundant information was discarded ,e.g., same biological processes showing as being affected by different databases). This analysis shows that DMR associated genes are mainly enriched in biological processes such as G-protein activation (comprising ~10% of the genes in that pathway), mitogen-activated protein kinase (MAPK) signaling (where five genes in our list participate) and purine ribonucleotide binding (where 14 genes in our list participate). P-and q- values of all significantly affected pathways are shown in Supplementary Table 3. In addition to these main affected pathways, less enriched pathways are shown in Supplementary Table 3. Of interest is also the appearance in the network of processes such as 'visual photo-transduction', 'opioid signaling', mRNA processing and cytoskeleton organization.

The network analysis performed with Reactome, in turn, shows that genes with altered DNA methylation in our list primarily target pathways in the immune system (Figure S2.B), followed by signal transduction pathways involved in opioid signaling, regulation of the photo-transduction cascade and G-protein activation (Figure S2.C). A less affected pathway was the 'metabolic', which showed effects in the sub-pathway 'inhibition of insulin secretion by adrenaline and noradrenaline'. A scheme summarizing the main pathways hypothetically affected is shown in Figure 6.

Discussion-

Stress has been reported to associate with DNA methylation specific alterations in brain. For example, infant rats exposed to parental maltreatment present long term DNA methylation and gene expression changes in the BDNF (brain-derived neurotrophic factor) gene in the frontal cortex (Roth et al., 2009). However, from the perspective of using epigenetic tools to determine the history of stress in live animals, it is of interest to determine whether epigenetic changes can also be observed in cell types of easy access such as blood cells.

A few studies have reported epigenetic changes in blood related to stress. For example, adult rats previously exposed to traumatic conditions during early life exhibit altered microRNA profile in the blood, brain and spermatozoids compared to non-traumatized individuals (Gapp et al., 2014). In humans (Malan-Muller et al., 2014) and monkeys (Provencal et al., 2012) DNA methylation in peripheral blood cells has been shown to be altered in correlation with previous stress. Since birds have nucleated RBCs, they represent an organism model in which DNA methylation can be measured in live individuals, and in an easily accessible and simple to purify cell-type.

The present study evaluates the effects of early life conditions on adult DNA methylation patterns in a farm animal. This was performed in RBCs of adult hens after they had been reared in groups exposed to different levels of environmental complexity. Avian blood contains nucleated RBCs, which allows for accurate epigenetic profiling because it is a cell type that is simple to purify and can be obtained from live animals. The aim was to identify in adult hens epigenetic profiles in RBCs associated with different rearing conditions. The rearing conditions to which hens were subjected in the current study cause long-term differences in fearfulness as indicated by differences in inhibition of behavior and avoidance of a human and a novel object in a novel test arena (Brantsaeter et al., 2016). Although we have not documented stress-related physiological differences between the treatment groups during the rearing phase (first 16 weeks of age), the fact that fear responses are per definition associated with physiological stress suggests that the rearing treatments induce distinct long-term alterations in the stress response. On the one hand, birds in the complex aviary environment are likely to be exposed to a higher degree of mild intermittent stress. On the other hand, confinement in the more barren cage environment may generate a sustained and long-term stress due to deprivation. Interestingly, evidence indicates that the aviary environment may be harsher and more challenging than the cage environment, as indicated by the fact that mortality of aviary-housed birds is normally twice as high as that of cage-housed birds (Janczak and Riber, 2015). In addition to fear responses, these rearing conditions also associate with different levels of cognitive capabilities observed later in life in birds from the same groups as in the present experiment (Tahamtani et al., 2015).

A number of genomic regions presented changes in RBCs DNA methylation between the different rearing conditions tested. These DMR are more present in regulatory regions and less present in intergenic regions (Figure 4). Such regulatory regions refer to promoters, promoter flanking regions, enhancers, CTCF binding sites, transcription factor binding sites, or open chromatin regions, based on the categorization within the VEP functional annotation tool (McLaren et al., 2010). It is well documented that epigenetic mechanisms, particularly DNA methylation, within these regions are major players in the regulation of gene expression (Bogdanovic et al., 2016; Wan and Bartolomei, 2008; Weber et al., 2007; Weber and Schubeler, 2007). Interestingly, most of our DMR are within these regions, and thus have the potential to directly affect gene expression. In addition, a great number of these DMR are present in intronic regions, which suggests these could have an involvement in intron retention and splicing, as DNA methylation has recently been reported to have an important role in these processes (Wong et al., 2017). DMR were absent in chromosomes 3, 9, 14, 18, 23, 32 and W. All the other chromosomes presented a fairly even distribution of DMRs, although chromosome 25 is the one that contained the highest number (Figure 4). The genes associated with these DMR were tested in pathway network analyses to determine whether they would significantly affect biological processes. It is needed to emphasize that this network analysis can only be a proxy to orient the research for functional relation of genes in connection to DMRs. Also, it is important to mention that in order to use Consensus PathDB the genes in the chicken genome had to be extrapolated to humans, since this tool does not accept the ENSEMBL chicken genome annotation. Reactome, however, accepts the input of chicken genes with the ENSEMBL identifier, but it is not as well connected to other databases as Consensus PathDB is. Therefore, these two tools were used to provide complementary information about our gene list.

We used Consensus PathDB and Reactome to inquire for biological pathways enriched by the genes found associated to the DMRs reported here. For this, we tested whether at least two of the genes in our list would belong to a single biological pathway previously described in the associated databases. Within Consensus PathDB we also performed a Gene Ontology analysis to determine possible common functional roles of these genes. Consensus PathDB analyses demonstrate that differentially

methylated genes are involved in pathways related to G-protein activation (in particular, involved in opioid response and the photo-transduction cascade), MAPK signaling and purine ribonucleoside binding (related to post-transcriptional processes). MAPK are known to regulate a wide array of cell functions relating to regulation of gene expression in cellular processes such as proliferation, differentiation, mitosis, apoptosis and survival (Pearson et al., 2001). Interestingly, MAPKs such as p38, MK2 and MK3 are known to mediate stress response, regulating the transcriptional activation of so-called 'immediate early genes' in mammalian cells (Ronkina et al., 2011). The involvement of purine ribonucleoside (i.e., AMP and GMP) binding has been given minor attention in research investigating stress responses. However, of interest is recent data showing the mediation of purine ribonucleoside binding in the antidepressant side-effects of phosphodiesterase inhibitors (i.e., etazolate, an anxiolytic drug; sildenafil, a drug used in the treatment of erectile dysfunction) in mice (Wang et al., 2014).

Pathway analysis with Reactome gave similar results, since equivalent signal transduction pathways were shown to be affected. The main pathway affected in Reactome was the immune system. A reason for this effect in the immune system could be that animals living in a confined space would exhibit higher levels of stress, which are known correlate with altered immune response. In humans, for example, individuals with a history of post-traumatic stress have compromised immune systems, with reduced number of lymphocytes and T cells, reduced natural killer cells activity, and reduced production of interferon gamma and interleukin-4 (Kawamura et al., 2001). Also, housing conditions have been correlated to decreased immune response in farm animals. For example, dairy calves housed in smaller stalls present reduced lymphocyte proliferation in comparison with calves in larger stalls (Ferrante V. et al., 1998). In mice, the bedding type is shown to influence the intestinal immune system (Sanford et al., 2002).

In addition, many sub-pathways were affected within the immune system. Altered signal transduction pathways include opioid signaling, regulation of the photo-transduction cascade, and G-protein activation. Interestingly, opioid signaling has for a long time been related to housing conditions in farm animals. For example, in pigs opioid receptor density is affected by the housing conditions and is

inversely correlated to stereotypic behavior duration (Zanella et al., 1996). Also in pigs, the expression of opioid receptors in the amygdala is substantially different between individuals maintained in enriched versus conventional housing environment (Kalbe and Puppe, 2010). Although not much research has been done on the role of opioids in chickens, it has been reported that opioid systems modulate social attachment and isolation stress (Sufka et al., 1994; Warnick et al., 2005). This is concordant with finding in rats showing that social isolation increases the responsiveness of the kappa opioid receptor (Karkhanis et al., 2016). What emerges as an interesting finding in the present paper is that the opioid system could be affected not only in the central nervous system but also in peripheral cells. Further research needs to be done to understand the role of peripheral opioids systems in the modulation of stress response. Although not many studies have focused on the correlation between photo-transduction and stress, research in chickens has shown that immune response varies with light cycles in a circadian fashion, controlled in part by the pineal gland, which among other cell types contain B-lymphocytes (Bailey et al., 2003). Vasotocin receptors, which belong to the G-protein receptor family, have been reported to mediate stress response in chickens. The recently characterized neuropeptides in this family (VT2R and VT4R) are known to be involved in stress response, particularly within the cephalic lobe of the anterior pituitary (Kuenzel et al., 2013). Again, how these neuronal effects translate to peripheral signaling is an interesting matter of future investigation.

In addition, the Reactome metabolic pathway showed some effects in the inhibition of insulin secretion by adrenaline and noradrenaline. Experiments with perfused (canine) pancreas show that insulin secretion is strongly inhibited by adrenaline or noradrenaline (Iversen, 1973). In turn, adrenaline and norepinephrine levels are known to vary not only due to stress (Henry, 1992; Ishibashi et al., 2013; Muller et al., 2013) but also in connection with the conditions under which animals are kept in captivity (Muller et al., 2013). For example in porpoises, free-ranging animals present higher blood levels of both adrenaline and noradrenaline than animals in rehabilitation or under human care (Muller et al., 2013). It is not surprising that high adrenaline or noradrenaline levels in free-ranging animals will lead to the inhibition of insulin and a concomitant rapid increase in circulatory glucose

levels, concordant with the high energy demands of animals living in free-ranging conditions. However, it is intriguing that such a mechanisms could be epigenetically regulated.

An interesting suggestion from our data is that a compromised immune system response could be imprinted in the epigenome of RBCs after animals are reared under specific conditions of stress. Since DNA methylation patterns are altered, it is suggested that the different rearing conditions leave an epigenetic mark in the red blood cells that will in turn affect the functioning of biological processes such as immune response, maybe in a permanent manner. Further experiments are needed to elucidate whether altered physiological measures of immune responses can correlate to developmentally-altered epigenetic patterns in farm animals.

The aim of the current study was to identify epigenetic profiles of early developmental stress-related environmental effects in RBCs. We identified distinguishable DNA methylation profiles relating to each treatment. The future goal is that the present results can be used as a proof-of-concept for the identification of epigenetic marks related to past stress conditions that occur in the production environment. Future experiments should evaluate whether sets of DMRs could constitute reliable 'epigenetic signatures' of specific and controlled stress conditions in extended populations of animals. The present study reports for the first time DNA methylation changes in RBCs of adult hens when reared in conditions of differing environmental complexity. We describe that these changes in DNA methylation associate with genes involved in biological functions such as immune response, and cell signaling related to MAPK, G-protein and opioid pathways. These results open interesting questions regarding the role of early life stimuli in altering epigenetic patterns that could be involved in these mechanisms. Moreover, questions also arise regarding the role RBCs play in G-protein and opioid pathways in stress response.

Acknowledgements

FP appreciates funding from CAPES (Brazilian government) for PhD research internship (PDSE, Programa de Doutourado-sanduíche no exterior) at Linköping University (Sweden). AMJ, JN and

MB acknowledge that parts of this study involving the use of live animals were funded by the Foundation for Research Levy on Agricultural Products (FFL), the Agricultural Agreement Research Fund (JA), and Animalia (Norwegian Meat and Poultry Research Centre) through the Research Council of Norway, grant number 207739. LLC is a recipient of a research productivity scholarship from CNPq (Brazilian government) and receives funding from FAPESP (Sao Paulo State, Brazil), grant 2014/08704-0. CGB and PJ appreciates funding from the European Research Council advanced grant 322206 ‘Genewell’ to PJ.

Author contributions

MB and AMJ conceived the animal treatments used in this study. MB and JN performed the experimental work in animals, including sample collection. MB, AMJ, CGB and PJ conceived the molecular experiments in this work. FP and CGB performed the molecular work, analyzed the data, and wrote the bulk of the manuscript. All authors contributed to the writing of the manuscript and critically reviewed the final versions. AMJ, PJ and LLC provided the main financial support for the experimental work and data analyses performed here.

Additional information

Competing financial interests: The authors declare no competing financial interests.

References

Andrew, S. (2010). FASTQC. A quality control tool for high throughput sequence data. *Available at: http://www.bioinformatics.babraham.ac.uk/projects/fastqc*, Date of access: Nov 2nd 2016.

Bailey, M. J., Beremand, P. D., Hammer, R., Bell-Pedersen, D., Thomas, T. L. and Cassone, V. M. (2003). Transcriptional profiling of the chick pineal gland, a photoreceptive circadian oscillator and pacemaker. *Mol Endocrinol* **17**, 2084-95.

Bogdanovic, O., Smits, A. H., de la Calle Mustienes, E., Tena, J. J., Ford, E., Williams, R., Senanayake, U., Schultz, M. D., Hontelez, S., van Kruijsbergen, I. et al. (2016). Active DNA demethylation at enhancers during the vertebrate phylotypic period. *Nat Genet* **48**, 417-26.

Brantsaeter, M., Nordgreen, J., Rodenburg, T. B., Tahamtani, F. M., Popova, A. and Janczak, A. M. (2016). Exposure to Increased Environmental Complexity during Rearing Reduces Fearfulness and Increases Use of Three-Dimensional Space in Laying Hens (Gallus gallus domesticus). *Front Vet Sci* **3**, 14.

Broom, D. M. (2010). Animal welfare: an aspect of care, sustainability, and food quality required by the public. *J Vet Med Educ* **37**, 83-8.

Catchen, J. M., Amores, A., Hohenlohe, P., Cresko, W. and Postlethwait, J. H. (2011). Stacks: building and genotyping Loci de novo from short-read sequences. *G3 (Bethesda)* **1**, 171-82.

Chavez, L., Jozefczuk, J., Grimm, C., Dietrich, J., Timmermann, B., Lehrach, H., Herwig, R. and Adjaye, J. (2010). Computational analysis of genome-wide DNA methylation during the differentiation of human embryonic stem cells along the endodermal lineage. *Genome Res* **20**, 1441-50.

Croft, D., O'Kelly, G., Wu, G., Haw, R., Gillespie, M., Matthews, L., Caudy, M., Garapati, P., Gopinath, G., Jassal, B. et al. (2011). Reactome: a database of reactions, pathways and biological processes. *Nucleic Acids Res* **39**, D691-7.

Cubas, P., Vincent, C. and Coen, E. (1999). An epigenetic mutation responsible for natural variation in floral symmetry. *Nature* **401**, 157-61.

Denham, J., Marques, F. Z., O'Brien, B. J. and Charchar, F. J. (2014). Exercise: putting action into our epigenome. *Sports Med* **44**, 189-209.

Dickman, M. J., Kucharski, R., Maleszka, R. and Hurd, P. J. (2013). Extensive histone post-translational modification in honey bees. *Insect Biochem Mol Biol* **43**, 125-37.

Dolinoy, D. C., Huang, D. and Jirtle, R. L. (2007). Maternal nutrient supplementation counteracts bisphenol A-induced DNA hypomethylation in early development. *Proc Natl Acad Sci U S A* **104**, 13056-61.

Down, T. A., Rakyan, V. K., Turner, D. J., Flicek, P., Li, H., Kulesha, E., Graf, S., Johnson, N., Herrero, J., Tomazou, E. M. et al. (2008). A Bayesian deconvolution strategy for immunoprecipitation-based DNA methylome analysis. *Nat Biotechnol* **26**, 779-85.

Elshire, R. J., Glaubitz, J. C., Sun, Q., Poland, J. A., Kawamoto, K., Buckler, E. S. and Mitchell, S. E. (2011). A Robust, Simple Genotyping-by-Sequencing (GBS) Approach for High Diversity Species. *PLoS One* **6**, e19379.

Fallahsharoudi, A., de Kock, N., Johnsson, M., Ubhayasekera, S. J., Bergquist, J., Wright, D. and Jensen, P. (2015). Domestication Effects on Stress Induced Steroid Secretion and Adrenal Gene Expression in Chickens. *Sci Rep* **5**, 15345.

Feil, R. and Fraga, M. F. (2011). Epigenetics and the environment: emerging patterns and implications. *Nat Rev Genet* **13**, 97-109.

Ferrante V., Canali E., Mattiello S., Verga M., Sacerdote P., Manfredi B. and A.E., P. (1998). Preliminary study on the effect of size of individual stall on the behavioural and immune reactions of dairy calves. *J. Anim. Feed Sci.* **7**, 29-36.

Fresard, L., Morisson, M., Brun, J. M., Collin, A., Pain, B., Minvielle, F. and Pitel, F. (2013). Epigenetics and phenotypic variability: some interesting insights from birds. *Genet Sel Evol* **45**, 16.

Gapp, K., Jawaid, A., Sarkies, P., Bohacek, J., Pelczar, P., Prados, J., Farinelli, L., Miska, E. and Mansuy, I. M. (2014). Implication of sperm RNAs in transgenerational inheritance of the effects of early trauma in mice. *Nat Neurosci* **17**, 667-9.

Glaubitz, J. C., Casstevens, T. M., Lu, F., Harriman, J., Elshire, R. J., Sun, Q. and Buckler, E. S. (2014). TASSEL-GBS: a high capacity genotyping by sequencing analysis pipeline. *PLoS One* **9**, e90346.

Goerlich, V. C., Natt, D., Elfwing, M., Macdonald, B. and Jensen, P. (2012). Transgenerational effects of early experience on behavioral, hormonal and gene expression responses to acute stress in the precocial chicken. *Horm Behav* **61**, 711-8.

Gu, H., Smith, Z. D., Bock, C., Boyle, P., Gnirke, A. and Meissner, A. (2011). Preparation of reduced representation bisulfite sequencing libraries for genome-scale DNA methylation profiling. *Nat Protoc* **6**, 468-81.

Guerrero-Bosagna, C. and Jensen, P. (2015). Optimized method for methylated DNA immuno-precipitation. *MethodsX* **2**, 432-9.

Guerrero-Bosagna, C. and Skinner, M. K. (2012). Environmentally induced epigenetic transgenerational inheritance of phenotype and disease. *Mol Cell Endocrinol* **354**, 3-8.

Guerrero-Bosagna, C. M., Sabat, P., Valdovinos, F. S., Valladares, L. E. and Clark, S. J. (2008). Epigenetic and phenotypic changes result from a continuous pre and post natal dietary exposure to phytoestrogens in an experimental population of mice. *BMC Physiol* **8**, 17.

Hendrix, G. (2015). General Management Guide for Dekalb White Commercial Layer. *Available at: http://www.isapoultry.com/~/media/Files/ISA/ISA%20product%20information/Dekalb/Parent%20Stock/General%20%20Management%20Guide%20Commercials%20Dekalb%20white.pdf2014*, Date of access: Nov 2nd 2016.

Henry, J. P. (1992). Biological basis of the stress response. *Integr Physiol Behav Sci* **27**, 66-83.

Ishibashi, M., Akiyoshi, H., Iseri, T. and Ohashi, F. (2013). Skin conductance reflects drug-induced changes in blood levels of cortisol, adrenaline and noradrenaline in dogs. *J Vet Med Sci* **75**, 809-13.

Iversen, J. (1973). Adrenergic receptors and the secretion of glucagon and insulin from the isolated, perfused canine pancreas. *J Clin Invest* **52**, 2102-16.

Janczak, A. M. and Riber, A. B. (2015). Review of rearing-related factors affecting the welfare of laying hens. *Poult Sci* **94**, 1454-69.

Jensen, P. (2014). Behaviour epigenetics – The connection between environment, stress and welfare. *Appl. Anim. Behav. Sci* **157**, 1-7.

Kain, K. H., Miller, J. W., Jones-Paris, C. R., Thomason, R. T., Lewis, J. D., Bader, D. M., Barnett, J. V. and Zijlstra, A. (2014). The chick embryo as an expanding experimental model for cancer and cardiovascular research. *Dev Dyn* **243**, 216-28.

Kalbe, C. and Puppe, B. (2010). Long-term cognitive enrichment affects opioid receptor expression in the amygdala of domestic pigs. *Genes Brain Behav* **9**, 75-83.

Kamburov, A., Stelzl, U., Lehrach, H. and Herwig, R. (2013). The ConsensusPathDB interaction database: 2013 update. *Nucleic Acids Res* **41**, D793-800.

Karkhanis, A. N., Rose, J. H., Weiner, J. L. and Jones, S. R. (2016). Early-Life Social Isolation Stress Increases Kappa Opioid Receptor Responsiveness and Downregulates the Dopamine System. *Neuropsychopharmacology* **41**, 2263-74.

Kawamura, N., Kim, Y. and Asukai, N. (2001). Suppression of cellular immunity in men with a past history of posttraumatic stress disorder. *Am J Psychiatry* **158**, 484-6.

Kuenzel, W. J., Kang, S. W. and Jurkevich, A. (2013). Neuroendocrine regulation of stress in birds with an emphasis on vasotocin receptors (VTRs). *Gen Comp Endocrinol* **190**, 18-23.

Langmead, B. and Salzberg, S. L. (2012). Fast gapped-read alignment with Bowtie 2. *Nat Methods* **9**, 357-9.

Li, H., Handsaker, B., Wysoker, A., Fennell, T., Ruan, J., Homer, N., Marth, G., Abecasis, G., Durbin, R. and Genome Project Data Processing, S. (2009). The Sequence Alignment/Map format and SAMtools. *Bioinformatics* **25**, 2078-9.

Lyko, F., Foret, S., Kucharski, R., Wolf, S., Falckenhayn, C. and Maleszka, R. (2010). The honey bee epigenomes: differential methylation of brain DNA in queens and workers. *PLoS Biol* **8**, e1000506.

Malan-Muller, S., Seedat, S. and Hemmings, S. M. (2014). Understanding posttraumatic stress disorder: insights from the methylome. *Genes Brain Behav* **13**, 52-68.

Manning, K., Tor, M., Poole, M., Hong, Y., Thompson, A. J., King, G. J., Giovannoni, J. J. and Seymour, G. B. (2006). A naturally occurring epigenetic mutation in a gene encoding an SBP-box transcription factor inhibits tomato fruit ripening. *Nat Genet* **38**, 948-52.

McLaren, W., Pritchard, B., Rios, D., Chen, Y., Flicek, P. and Cunningham, F. (2010). Deriving the consequences of genomic variants with the Ensembl API and SNP Effect Predictor. *Bioinformatics* **26**, 2069-70.

Morgan, K. N. and Tromborg, C. T. (2006). Sources of stressa in captivity. *Appl Anim Behav Sci* **102**, 262-302.

Muller, S., Lehnert, K., Seibel, H., Driver, J., Ronnenberg, K., Teilmann, J., van Elk, C., Kristensen, J., Everaarts, E. and Siebert, U. (2013). Evaluation of immune and stress status in harbour porpoises (Phocoena phocoena): can hormones and mRNA expression levels serve as indicators to assess stress? *BMC Vet Res* **9**, 145.

OECD-FAO. (2015). Agricultural Outlook. *Available at: http://www.fao.org/3/a-i4738e.pdf*, Date of access: Nov 2nd 2016.

Olanrewaju, H. A., Thaxton, J. P., Dozier III, W. A., Purswell, J., Roush, W. B. and Branton, S. L. (2006). A Review of Lighting Programs for Broiler Production. *Int. J. Poult. Sci.* **5**, 301-308.

Pearson, G., Robinson, F., Beers Gibson, T., Xu, B. E., Karandikar, M., Berman, K. and Cobb, M. H. (2001). Mitogen-activated protein (MAP) kinase pathways: regulation and physiological functions. *Endocr Rev* **22**, 153-83.

Pértille, F., Guerrero-Bosagna, C., da Silva, V., Boschiero, C., Nunes, J., Ledur, M., Jensen, P. and Coutinho, L. (2016). High-throughput and Cost-effective chicken genotyping using Next-Generation Sequencing. *Submitted article*.

Poland, J. A. and Rife, T. W. (2012). Genotyping-by-Sequencing for Plant Breeding and Genetics. *The Plant Genome* **5**.

Provencal, N., Suderman, M. J., Guillemin, C., Massart, R., Ruggiero, A., Wang, D., Bennett, A. J., Pierre, P. J., Friedman, D. P., Cote, S. M. et al. (2012). The signature of maternal rearing in the methylome in rhesus macaque prefrontal cortex and T cells. *J Neurosci* **32**, 15626-42.

Ronkina, N., Menon, M. B., Schwermann, J., Arthur, J. S., Legault, H., Telliez, J. B., Kayyali, U. S., Nebreda, A. R., Kotlyarov, A. and Gaestel, M. (2011). Stress induced gene expression: a direct role for MAPKAP kinases in transcriptional activation of immediate early genes. *Nucleic Acids Res* **39**, 2503-18.

Rostagno, M. H. (2009). Can stress in farm animals increase food safety risk? *Foodborne Pathog Dis* **6**, 767-76.

Roth, T. L., Lubin, F. D., Funk, A. J. and Sweatt, J. D. (2009). Lasting epigenetic influence of early-life adversity on the BDNF gene. *Biol Psychiatry* **65**, 760-9.

Rubin, C. J., Zody, M. C., Eriksson, J., Meadows, J. R., Sherwood, E., Webster, M. T., Jiang, L., Ingman, M., Sharpe, T., Ka, S. et al. (2010). Whole-genome resequencing reveals loci under selection during chicken domestication. *Nature* **464**, 587-91.

Sanford, A. N., Clark, S. E., Talham, G., Sidelsky, M. G. and Coffin, S. E. (2002). Influence of bedding type on mucosal immune responses. *Comp Med* **52**, 429-32.

Savory, C. J. and Lariviere, J. (2000). Effects of qualitative and quantitative food restriction treatments on feeding motivational state and general activity level of growing broiler breeders. *Appl Anim Behav Sci* **69**, 135-147.

Seong, K. H., Li, D., Shimizu, H., Nakamura, R. and Ishii, S. (2011). Inheritance of stress-induced, ATF-2-dependent epigenetic change. *Cell* **145**, 1049-61.

Skinner, M. K., Manikkam, M. and Guerrero-Bosagna, C. (2010). Epigenetic transgenerational actions of environmental factors in disease etiology. *Trends Endocrinol Metab* **21**, 214-22.

Sufka, K. J., Hughes, R. A., McCormick, T. M. and Borland, J. L. (1994). Opiate effects on isolation stress in domestic fowl. *Pharmacol Biochem Behav* **49**, 1011-5.

Susiarjo, M., Sasson, I., Mesaros, C. and Bartolomei, M. S. (2013). Bisphenol a exposure disrupts genomic imprinting in the mouse. *PLoS Genet* **9**, e1003401.

Tahamtani, F. M., Nordgreen, J., Nordquist, R. E. and Janczak, A. M. (2015). Early Life in a Barren Environment Adversely Affects Spatial Cognition in Laying Hens (Gallus gallus domesticus). *Front Vet Sci* **2**, 3.

Teperek-Tkacz, M., Pasque, V., Gentsch, G. and Ferguson-Smith, A. C. (2011). Epigenetic reprogramming: is deamination key to active DNA demethylation? *Reproduction* **142**, 621-32.

Wan, L. B. and Bartolomei, M. S. (2008). Regulation of imprinting in clusters: noncoding RNAs versus insulators. *Adv Genet* **61**, 207-23.

Wang, C., Zhang, J., Lu, Y., Lin, P., Pan, T., Zhao, X., Liu, A., Wang, Q., Zhou, W. and Zhang, H. T. (2014). Antidepressant-like effects of the phosphodiesterase-4 inhibitor etazolate and phosphodiesterase-5 inhibitor sildenafil via cyclic AMP or cyclic GMP signaling in mice. *Metab Brain Dis* **29**, 673-82.

Warnick, J. E., McCurdy, C. R. and Sufka, K. J. (2005). Opioid receptor function in social attachment in young domestic fowl. *Behav Brain Res* **160**, 277-85.

Weber, M., Hellmann, I., Stadler, M. B., Ramos, L., Paabo, S., Rebhan, M. and Schubeler, D. (2007). Distribution, silencing potential and evolutionary impact of promoter DNA methylation in the human genome. *Nat Genet* **39**, 457-66.

Weber, M. and Schubeler, D. (2007). Genomic patterns of DNA methylation: targets and function of an epigenetic mark. *Curr Opin Cell Biol* **19**, 273-80.

Wong, J. J., Gao, D., Nguyen, T. V., Kwok, C. T., van Geldermalsen, M., Middleton, R., Pinello, N., Thoeng, A., Nagarajah, R., Holst, J. et al. (2017). Intron retention is regulated by altered MeCP2-mediated splicing factor recruitment. *Nat Commun* **8**, 15134.

Zanella, A. J., Broom, D. M., Hunter, J. C. and Mendl, M. T. (1996). Brain opioid receptors in relation to stereotypies, inactivity, and housing in sows. *Physiol Behav* **59**, 769-75.

Zannas, A. S. and West, A. E. (2014). Epigenetics and the regulation of stress vulnerability and resilience. *Neuroscience* **264**, 157-70.

Zhang, Q., Yoon, Y., Yu, Y., Parnell, E. J., Garay, J. A., Mwangi, M. M., Cross, F. R., Stillman, D. J. and Bai, L. (2013). Stochastic expression and epigenetic memory at the yeast HO promoter. *Proc Natl Acad Sci U S A* **110**, 14012-7.

Zhbannikov, I. Y., Hunter, S. S. and Settles, M. L. (2013). SEQYCLEAN User Manual. *Available at: https://github.com/ibest/seqyclean*, Date of access: Nov 2nd 2016.

Figures

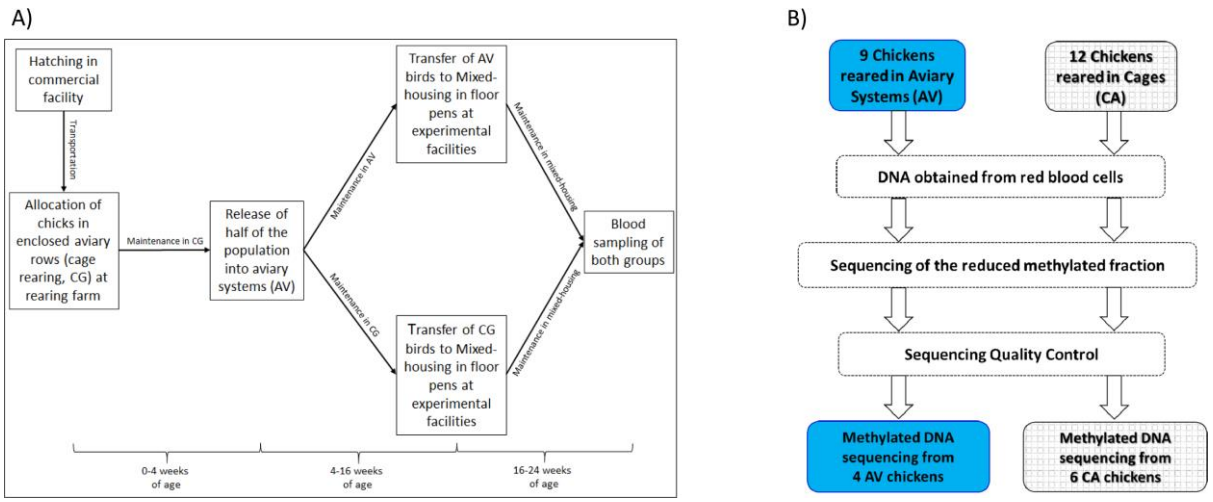

Figure 1- A) Schematic representation of the housing conditions in the two experimental treatments.

B) Diagram summarizing the processing of samples from individuals in each treatment group.

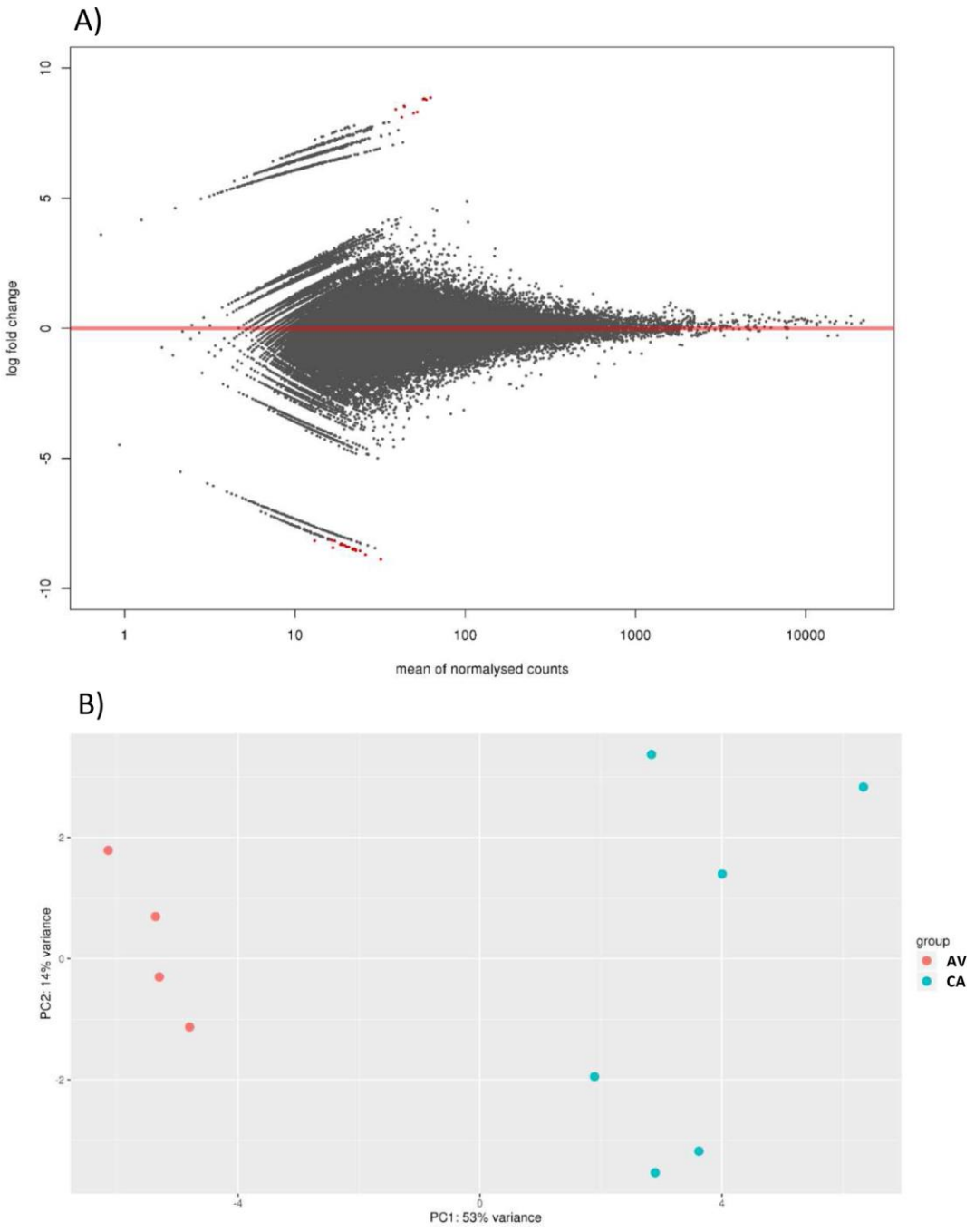

Figure 2- A) MA plot showing the log-fold change of AV/CA counts (changes in DNA methylation) per 300 bp genomic windows against the normalized window counts. Windows with significant changes ($P < 0.0005$) between experimental groups ($N_{AV} = 4$; $N_{CA} = 6$) are depicted as red dots. B) Principal components analysis (PCA) performed using the genomic windows with significant differences in counts ($P < 0.0005$) between the AV and CA groups.

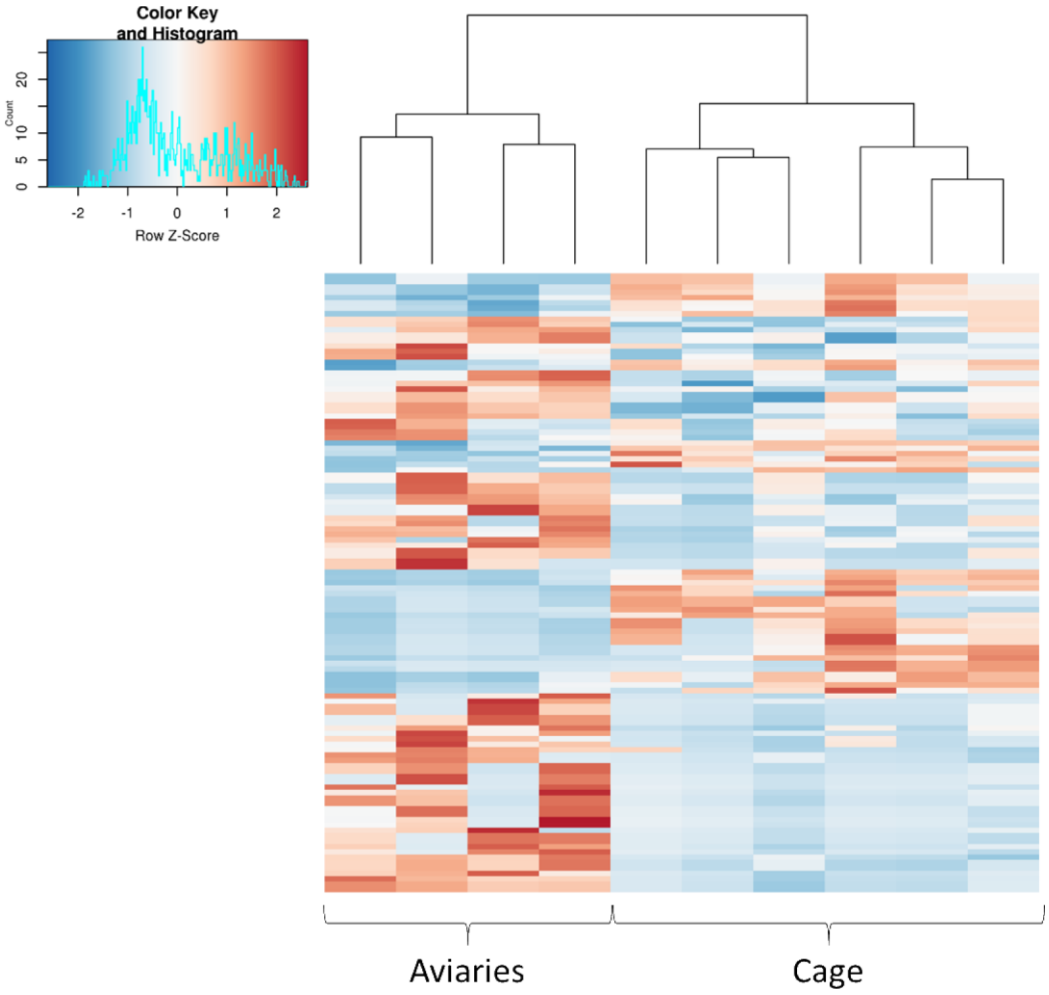

Figure 3- Heat map showing the genomic windows with significant changes in DNA methylation between experimental groups ($P < 0.0005$; $N_{AV} = 4$; $N_{CA} = 6$).

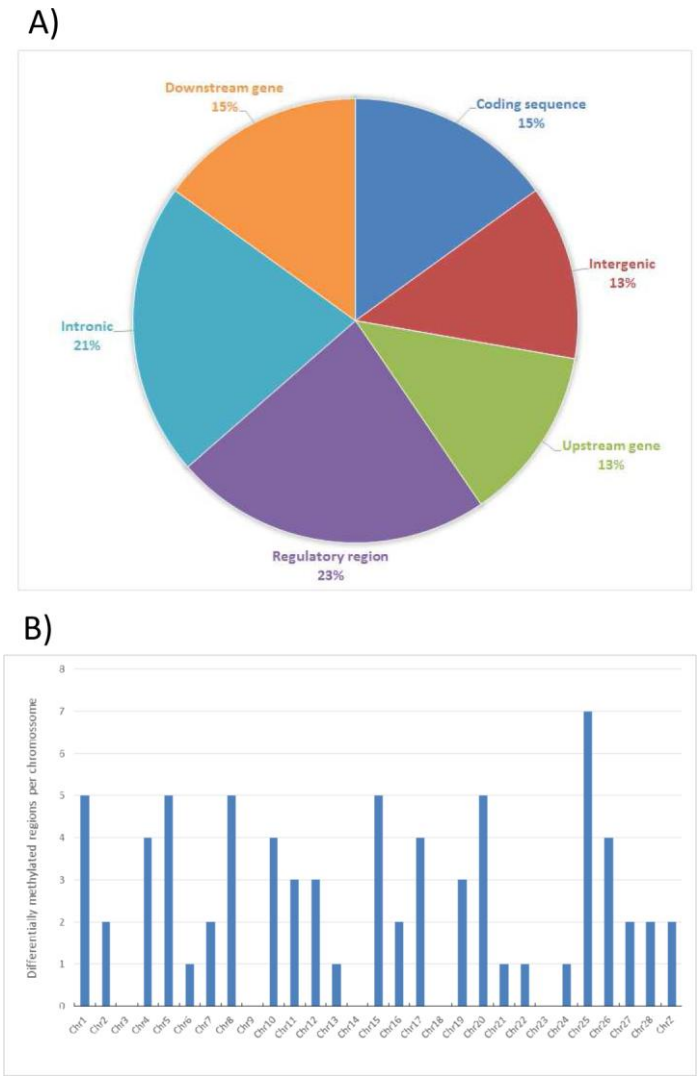

Figure 4- Location of DMRs regarding (a) nearby or associated genes, and (b) chromosomes.

Figure 5- Fold change representation of DMR-associated genes or intergenic regions between the experimental groups.

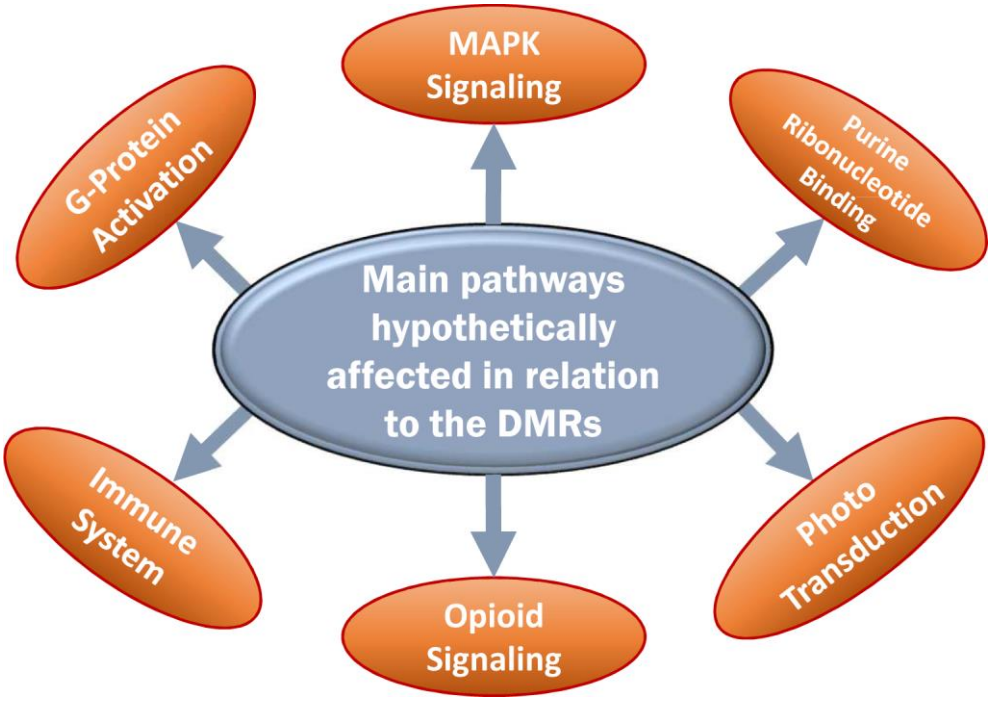

Figure 6- Schematic representation of the main biological pathways hypothetically affected by the DMRs found between the experimental groups (i.e., AV and CA).

Figure S1- Relation between Individual average coverage (S.Cov) and percentage of the genome covered (%Cov). The size of the balloons represent the cut-off index defined as %Cov/S.Cov * 100.

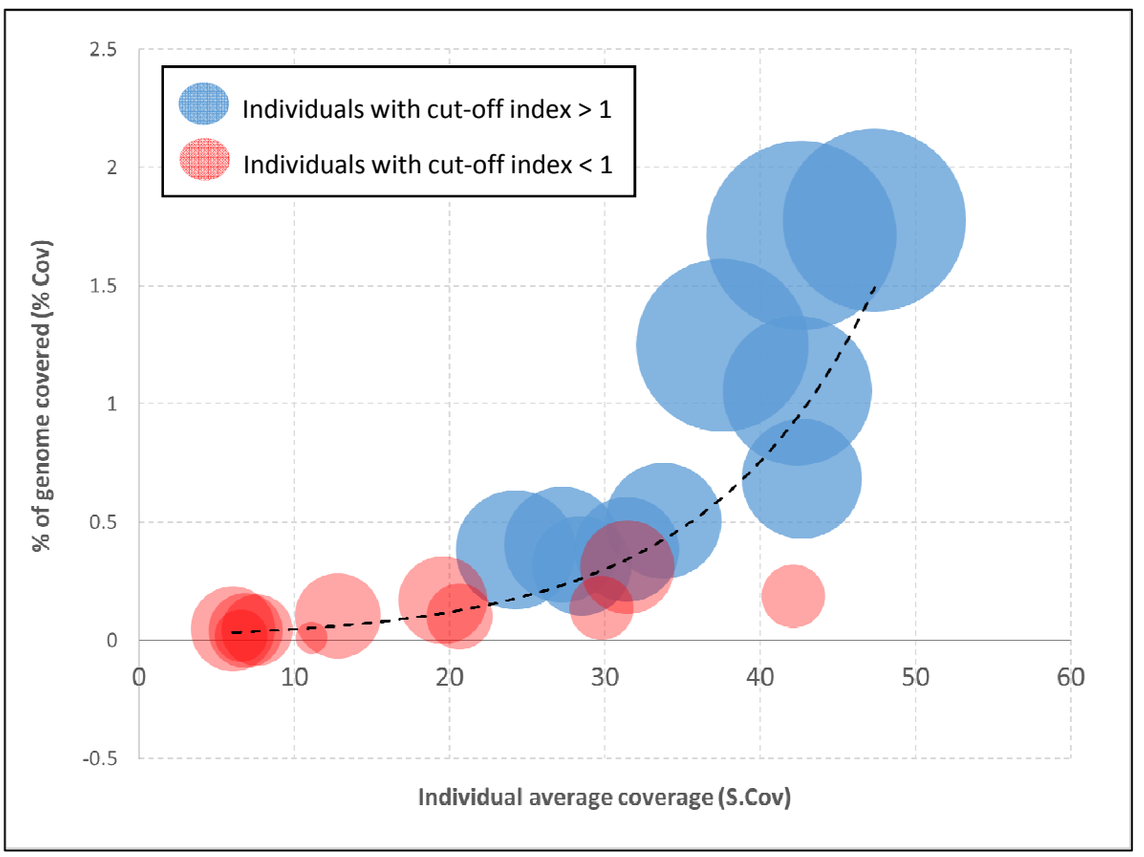

	Coverage	Number of bases covered	Unique nucleotides sequenced	% of the Chicken Genome Covered	Cut-off index	Passed cut-off index?
RJF_AV163_cleaned_sorted.bam	42.65	785050701	18407679	1.71	4.02	Y
RJF_C165_cleaned_sorted.bam	47.36	904820256	19107134	1.78	3.75	Y
RJF_C167_cleaned_sorted.bam	37.56	503891013	13415736	1.25	3.32	Y
RJF_AV171_cleaned_sorted.bam	42.39	481170980	11350889	1.06	2.49	Y
RJF_C175_cleaned_sorted.bam	42.69	313281350	7337848	0.68	1.60	Y
RJF_AV170_cleaned_sorted.bam	24.25	100141920	4129700	0.38	1.58	Y
RJF_C172_cleaned_sorted.bam	33.79	183302789	5424893	0.50	1.49	Y
RJF_AV176_cleaned_sorted.bam	27.24	118755610	4359012	0.41	1.49	Y
RJF_C174_cleaned_sorted.bam	31.39	129808223	4135284	0.38	1.23	Y
RJF_C178_cleaned_sorted.bam	28.51	96777429	3394282	0.32	1.11	Y
RJF_C164_cleaned_sorted.bam	31.43	104579349	3327659	0.31	0.99	N
RJF_C181_cleaned_sorted.bam	19.55	35561207	1819164	0.17	0.87	N
RJF_C182_cleaned_sorted.bam	12.80	14262264	1114109	0.10	0.81	N
RJF_C180_cleaned_sorted.bam	6.04	3134870	519214	0.05	0.80	N
RJF_C184_cleaned_sorted.bam	6.85	3145741	458998	0.04	0.62	N
RJF_AV179_cleaned_sorted.bam	7.60	3560878	468367	0.04	0.57	N
RJF_AV186_cleaned_sorted.bam	20.64	22434655	1086845	0.10	0.49	N
RJF_C173_cleaned_sorted.bam	29.78	43589534	1463841	0.14	0.46	N
RJF_AV177_cleaned_sorted.bam	42.13	84819706	2013414	0.19	0.44	N
RJF_AV166_cleaned_sorted.bam	6.57	1426214	217137	0.02	0.31	N
RJF_AV169_cleaned_sorted.bam	11.12	1505151	135301	0.01	0.11	N
Average	**26.30200667**	**187381897.1**	**4937452.683**	**0.45931501**	**1.36**	

***Figure S2*- A)** Network analysis performed with Consensus PathDB showing how the DMR associated genes relate to biological pathways and gene ontology information. Significantly enriched pathways and GO terms are shown. Significance values for the pathway over-representation analysis and enriched GO terms are shown in Supplementary Table 3. The numbers within circles correspond to DMR-associated genes within a specific affected biological pathway (circles with blue annotations) or GO terms (circles with pink annotations). The size of the circles correspond to the total number of genes in the database for that specific pathway. **B)** and **C)** Network analysis performed with Reactome showing how the DMR associated genes relate to biological pathways. Significantly enriched pathways are shown for the immune system **(B)** and signal transduction **(C)**.

A)

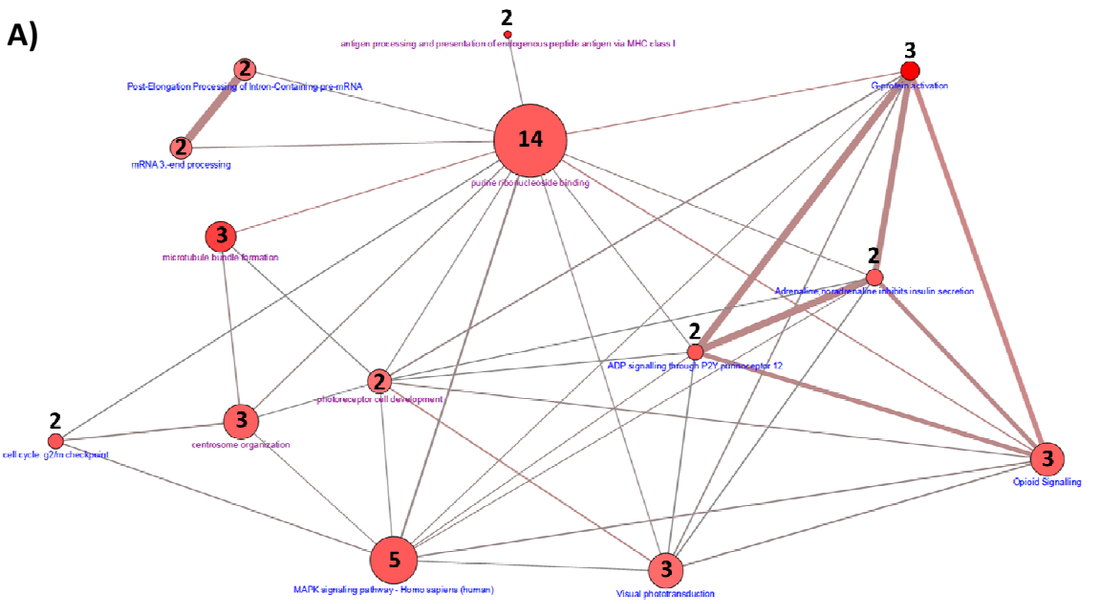

B)

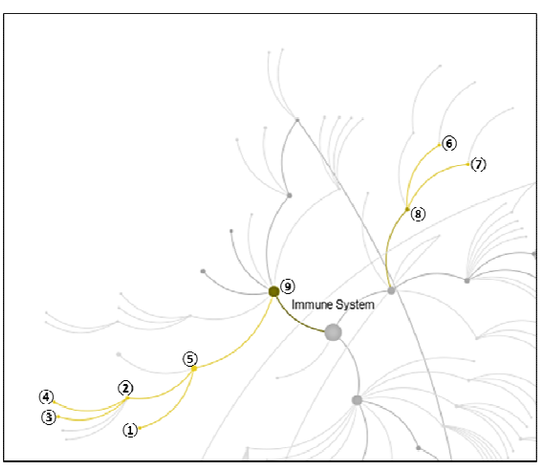

1- Antigen Presentation: Folding, assembly and peptide loading of class I MHC
2- Antigen processing-Cross presentation
3- ER-Phagosome pathway
4- Endosomal/Vacuolar pathway
5- Class I MHC mediated antigen processing & presentation
6- Interferon alpha/beta signaling
7- Interferon gamma signaling
8- Interferon Signaling
9- Adaptive Immune System

C)

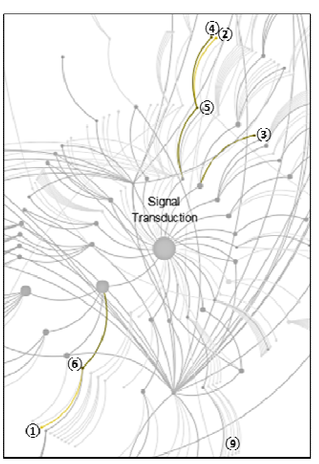

1- G-protein activation
2- Activation of the phototransduction cascade
3- Nerve growth factor (NGF) processing
4- Inactivation, recovery and regulation of the phototransduction cascade
5- The phototransduction cascade
6- Opioid Signaling

SUPPLEMENTARY TABLE 1

	Location	Gene	SYMBOL	edgeR logFC	edgeR logCPM	edgeR p-value	edgeR adj p-value
1	chr1:1244701-1245000	ENSGALG00000008449	novel gene	4.448	3.344	0.005	4.69E-03
2	chr1:1245001-1245300			4.448	3.344	0.005	4.69E-03
3	chr1:44775901-44776200	ENSGALG00000011297	CRADD	-1.373	6.134	0.003	2.79E-03
4	chr1:81671101-81671400	-	-	2.877	4.270	0.002	1.77E-03
5	chr1:81671401-81671700			2.877	4.270	0.002	1.77E-03
6	chr1:143647201-143647500	-	-	2.179	4.363	0.002	2.32E-03
7	chr1:143647501-143647800			2.179	4.363	0.002	2.32E-03
8	chr1:193971001-193971300	ENSGALG00000009114	DGAT2	2.541	3.400	0.004	4.08E-03
9	chr1:193971301-193971600			2.541	3.400	0.004	4.08E-03
10	chr1:193971601-193971900			3.195	3.370	0.004	3.73E-03
11	chr2:223501-223800	ENSGALG00000013341	AGAP3	3.053	3.326	0.003	2.74E-03
12	chr2:112513801-112514100	ENSGALG00000015450	RAB2A	-3.924	4.005	0.003	3.37E-03
13	chr4:13297201-13297500	ENSGALG00000008006	CAPN6	2.767	3.510	0.003	3.14E-03
14	chr4:13429201-13429500	-	-	-1.567	4.940	0.003	2.67E-03
15	chr4:34189801-34190100	ENSGALG00000010291 ENSGALG00000010298	RBPMS; DCTN6	2.286	4.055	0.003	3.36E-03
16	chr4:34190101-34190400			2.557	3.982	0.003	2.71E-03
17	chr4:44742601-44742900	ENSGALG00000010893	FGF5	-2.695	4.638	0.000	2.65E-04
18	chr5:402001-402300	ENSGALG00000013298	CPSF7	3.572	3.779	0.002	1.88E-03
		ENSGALG00000022369	TMEM216				
		ENSGALG00000025756	TMEM138				
19	chr5:5731501-5731800	-	-	-0.713	8.232	0.003	3.36E-03
20	chr5:5731801-5732100			-0.712	8.514	0.002	1.82E-03
21	chr5:43370101-43370400	ENSGALG00000010680	TTC7B	3.802	3.585	0.000	4.92E-04
22	chr5:43370401-43370700			3.802	3.585	0.000	4.92E-04
23	chr5:56258101-56258400	ENSGALG00000012203	SAMD4A	-1.651	5.633	0.001	1.43E-03
24	chr5:56258401-56258700			-1.651	5.633	0.001	1.43E-03
25	chr5:57753301-57753600	ENSGALG00000012321	MAP4K5	-5.357	4.037	0.001	5.13E-04
26	chr5:57753601-57753900			-5.385	4.055	0.000	4.59E-04
27	chr6:27634201-27634500	ENSGALG00000025403	MIR1815	3.831	3.561	0.003	2.92E-03
28	chr6:27634501-27634800			3.831	3.561	0.003	2.92E-03
29	chr7:10155301-10155600	-	-	3.461	3.442	0.002	2.22E-03
30	chr7:10155601-10155900			3.461	3.442	0.002	2.22E-03
31	chr7:34455901-34456200	-	-	3.254	3.374	0.001	1.40E-03
32	chr7:34456201-34456500			3.254	3.374	0.001	1.40E-03
33	chr7:34456501-34456800	ENSGALG00000012475	novel gene	3.494	3.455	0.001	1.38E-03
34	chr8:3895201-3895500	-	-	2.440	3.704	0.002	1.61E-03
		ENSGALG00000010226	MUTYH				

35	chr8:19935901-19936200	ENSGALG00000010228	TOE1	1.891	4.176	0.005	4.58E-03
		ENSGALG00000023348	HPDL				
36	chr8:27597601-27597900	ENSGALG00000026591	GNG12	-1.819	4.950	0.002	2.49E-03
		ENSGALG00000025977	GADD45A				
37	chr8:27652201-27652500	ENSGALG00000011238	WLS	4.908	3.584	0.004	3.80E-03
		ENSGALG00000027802	gga-mir-6653				
38	chr8:28043701-28044000	-	-	-2.832	4.513	0.003	3.01E-03
39	chr10:2100301-2100600	ENSGALG00000001449	STRA6	-2.742	4.917	0.004	4.00E-03
		ENSGALG00000021525	ISLR				
		ENSGALG00000029151	novel gene				
40	chr10:12681001-12681300	-	-	4.800	3.523	0.004	3.92E-03
41	chr10:12681301-12681600	-	-	4.616	3.435	0.005	4.78E-03
42	chr10:19580401-19580700	ENSGALG00000008315 ENSGALG00000008336	UNC45A; MAN2A2	1.612	5.653	0.000	2.52E-04
43	chr10:19580701-19581000			1.708	5.559	0.000	1.90E-04
44	chr10:19592401-19592700	ENSGALG00000008340 ENSGALG00000008341	FES; FURIN	3.584	3.748	0.002	1.99E-03
45	chr10:19592701-19593000			3.584	3.748	0.002	1.99E-03
46	chr11:453601-453900	ENSGALG00000000904	USB1	3.478	3.400	0.004	4.02E-03
		ENSGALG00000000999	ZNF319				
		ENSGALG00000001011	CNGB1				
47	chr11:17139901-17140200	ENSGALG00000014284	GSE1	-5.359	4.016	0.003	3.01E-03
48	chr11:17140201-17140500			-5.359	4.016	0.003	3.01E-03
49	chr11:19161901-19162200	ENSGALG00000000802	DHODH	3.019	3.598	0.002	1.81E-03
		ENSGALG00000000811	IST1				
		ENSGALG00000000787	DHX38				
50	chr12:3190201-3190500	ENSGALG00000004639	GNAI2	2.362	4.114	0.005	4.95E-03
		ENSGALG00000013370	SEMA3F				
		ENSGALG00000028697	GNAT1				
51	chr12:5752201-5752500	-	-	-2.520	4.337	0.004	4.40E-03
52	chr12:5752501-5752800			-2.549	4.034	0.001	7.62E-04
53	chr12:11534101-11534400	-	-	-1.405	5.706	0.003	3.14E-03
54	chr12:11534401-11534700			-1.338	5.596	0.004	3.93E-03
55	chr13:15793201-15793500	ENSGALG00000006569	novel gene	2.434	4.351	0.005	4.97E-03

56	chr13:15793501-15793800	ENSGALG00000006569	novel gene	2.551	4.488	0.002	1.99E-03
57	chr15:2566201-2566500	ENSGALG00000002272	NOC4L	4.472	3.349	0.003	3.14E-03
		ENSGALG00000002336	RP11-2C24.9				
58	chr15:7104601-7104900	-	-	-3.205	4.148	0.004	3.67E-03
59	chr15:9882901-9883200	ENSGALG00000007396	TAOK3	2.858	3.697	0.001	9.83E-04
60	chr15:10068901-10069200	ENSGALG00000007720	AIFM3	1.460	4.850	0.004	4.38E-03
		ENSGALG00000028023	C14ORF166B				
		ENSGALG00000026902	P2RX6				
61	chr15:10800301-10800600	ENSGALG00000007781	GAL3ST1	-1.368	5.310	0.004	4.14E-03
		ENSGALG00000007840	RP4-539M6.19				
62	chr16:70501-70800	ENSGALG00000000178 ENSGALG00000000181 ENSGALG00000026269	BF1; novel gene; TAP1	2.832	4.523	0.001	8.84E-04
63	chr16:70801-71100			2.832	4.523	0.001	8.84E-04
64	chr16:219901-220200	ENSGALG00000019836 ENSGALG00000028962	ZNF692 novelgene	-5.336	4.053	0.003	2.77E-03
65	chr16:220201-220500			-5.393	4.088	0.002	2.42E-03
66	chr17:168901-169200	ENSGALG00000019837	KIFC1	1.344	4.824	0.005	4.74E-03
67	chr17:8289901-8290200	ENSGALG00000001595 ENSGALG00000001620	PHF19; CUTA	-3.805	5.124	0.001	8.25E-04
68	chr17:8290201-8290500			-3.677	3.935	0.001	1.25E-03
69	chr17:8550001-8550300	ENSGALG00000001419	DAB2IP	2.939	4.030	0.004	3.58E-03
70	chr17:8550301-8550600			2.939	4.030	0.004	3.58E-03
71	chr17:9845701-9846000	-	-	-5.019	3.840	0.002	1.58E-03
72	chr19:4471201-4471500	ENSGALG00000002186 ENSGALG00000002212	UNC45B; RAD51D	2.321	3.861	0.002	2.13E-03
73	chr19:4471501-4471800			2.321	3.861	0.002	2.13E-03
74	chr19:4753501-4753800	ENSGALG00000002312	TMEM132E	1.650	4.849	0.003	2.50E-03
75	chr19:4753801-4754100			1.669	4.859	0.003	2.59E-03
76	chr19:8303401-8303700	-	-	4.901	3.525	0.001	9.14E-04
77	chr19:8303701-8304000			4.901	3.525	0.001	9.14E-04
78	chr20:2325901-2326200	-	-	-4.852	4.715	0.001	7.05E-04
79	chr20:2326201-2326500			-4.115	4.730	0.003	2.62E-03
80	chr20:8868601-8868900	-	-	3.123	3.889	0.000	4.05E-04
81	chr20:9458401-9458700	ENSGALG00000005932	MYT1	-3.928	4.105	0.005	4.53E-03
82	chr20:11843101-11843400	ENSGALG00000007636	PCK1	-2.591	4.055	0.001	1.37E-03
83	chr20:11843401-11843700			-2.453	3.975	0.002	2.27E-03
84	chr20:11844601-11844900			-2.149	4.166	0.003	2.82E-03
85	chr20:11844901-11845200			-2.149	4.166	0.003	2.82E-03

86	chr21:4398301-4398600	ENSGALG00000027085	CROCC	1.579	5.808	0.000	4.36E-04
87	chr22:1246501-1246800	ENSGALG00000000402	LOXL2	-1.682	5.492	0.002	1.87E-03
		ENSGALG00000000405	R3HCC1				
88	chr22:1246801-1247100			-1.724	5.320	0.003	2.83E-03
89	chr24:2467801-2468100	ENSGALG00000001450	IGSF9B	3.291	3.378	0.004	3.57E-03
90	chr25:15301-15600	ENSGALG00000009011	SMG5	1.640	4.771	0.004	3.87E-03
91	chr25:15601-15900			1.640	4.771	0.004	3.87E-03
92	chr25:209701-210000	ENSGALG00000000443	novel gene	1.467	7.140	0.001	1.06E-03
93	chr25:210001-210300			1.954	6.799	0.000	3.49E-05
94	chr25:225301-225600	-	-	2.562	5.493	0.002	2.38E-03
95	chr25:225601-225900			2.420	5.586	0.002	1.78E-03
96	chr25:234901-235200	-	-	2.406	5.405	0.004	4.09E-03
97	chr25:235201-235500			2.394	5.426	0.004	3.86E-03
98	chr25:243301-243600	-	-	1.441	6.808	0.001	5.96E-04
99	chr25:660001-660300	ENSGALG00000027046	novel gene	3.421	3.810	0.005	4.91E-03
100	chr25:1675201-1675500	ENSGALG00000028854	DUSP23	1.213	5.974	0.004	4.41E-03
		ENSGALG00000022137	CRP				
101	chr25:1675501-1675800	ENSGALG00000027054 ENSGALG0000002879	novel gene; CADM3	1.213	5.974	0.004	4.41E-03
102	chr26:648601-648900	ENSGALG00000000362	NAV1	-1.825	4.777	0.005	4.69E-03
		ENSGALG00000028854	DUSP23				
103	chr26:1633201-1633500	ENSGALG00000000583	SOX13	3.188	3.594	0.002	2.18E-03
104	chr26:1633501-1633800			3.188	3.594	0.002	2.18E-03
105	chr26:1707301-1707600	ENSGALG00000000587	PLEKHA6	1.772	4.710	0.002	1.77E-03
106	chr26:4467901-4468200	-	-	-3.344	3.754	0.004	4.25E-03
107	chr27:2586001-2586300	ENSGALG00000000478	TANC2	3.125	3.321	0.005	4.69E-03
108	chr27:4113601-4113900	ENSGALG00000025788	CACNB1	3.252	3.461	0.004	4.33E-03
109	chr28:2780701-2781000	ENSGALG00000026231	ARID3A	-5.524	4.143	0.001	1.14E-03
110	chr28:2781001-2781300			-5.524	4.143	0.001	1.14E-03
111	chr28:3127801-3128100	ENSGALG00000024298	ADAMTSL5	2.225	3.991	0.003	3.27E-03
		ENSGALG00000026384	PCSK4				
112	chrZ:1446301-1446600	-	-	3.788	3.612	0.003	2.86E-03
123	chrZ:1446601-1446900			3.707	3.576	0.004	3.74E-03
114	chrZ:56827201-56827500	ENSGALG00000014684	ERAP1	1.661	4.443	0.003	2.79E-03
115	chrZ:56827501-56827800			1.661	4.443	0.003	2.79E-03

SUPPLEMENTARY TABLE 2

	Merged windows with differential methylation	CpGs within the merged window	DMR within or near gene		Position regarding gene
			ENSEMBL name	Gene symbol	
1	chr1:1244701-1245300	5	ENSGALG00000008449	Novel gene (1)	coding sequence ; intronic ; regulatory region
2	chr1:44775901-44776200	12	ENSGALG00000011297	CRADD	intronic ; regulatory region
3	chr1:81671101-81671700	10	--	Intergenic region (1)	intergenic
4	chr1:143647201-143647800	29	--	Intergenic region (2)	intergenic
5	chr1:193971001-193971900	36	ENSGALG00000009114	DGAT2	upstream gene
6	chr2:223501-223800	19	ENSGALG00000013341	AGAP3	intronic ; regulatory region
7	chr2:112513801-112514100	6	ENSGALG00000015450	RAB2A	upstream gene
8	chr4:13297201-13297500	4	ENSGALG00000008006	CAPN6	intronic ; regulatory region
9	chr4:13429201-13429500	11	--	Intergenic region (3)	intergenic
			ENSGALG00000010298	DCTN6	downstream gene
10	chr4:34189801-34190400	20	ENSGALG00000010291	RBPMS	coding sequence ; intronic ; regulatory region
11	chr4:44742601-44742900	14	ENSGALG00000010893	FGF5	coding sequence ; intronic ; regulatory region
12	chr5:402001-402300	10	ENSGALG00000013298	CPSF7	downstream gene
			ENSGALG00000022369	TMEM216	upstream gene
			ENSGALG00000025756	TMEM138	coding sequence ; intronic ; regulatory region
			ENSGALG00000028882	Novel gene (2)	upstream gene
13	chr5:5731501-5732100	29	--	Intergenic region (4)	intergenic
14	chr5:43370101-43370700	10	ENSGALG00000010680	TTC7B	intronic ; regulatory region
15	chr5:56258101-56258700	34	ENSGALG00000012203	SAMD4A	intronic ; regulatory region
16	chr5:57753301-57753900	6	ENSGALG00000012321	MAP4K5	upstream gene
17	chr6:27634201-27634800	3	ENSGALG00000025403	MIR1815	upstream gene
18	chr7:10155301-10155900	13	--	Intergenic region (5)	intergenic
19	chr7:34455901-34456800	20	--	Intergenic region (6)	intergenic
			ENSGALG00000012475	Novel gene (3)	downstream gene
20	chr8:3895201-3895500	7	--	Intergenic region (7)	intergenic
21	chr8:19935901-19936200	3	ENSGALG00000010226	MUTYH	coding sequence ; intronic ; regulatory region
			ENSGALG00000010228	TOE1	upstream gene
			ENSGALG00000023348	HPDL	downstream gene
22	chr8:27597601-27597900	8	ENSGALG00000026591	GNG12	coding sequence ; intronic ; regulatory region
			ENSGALG00000025977	GADD45A	downstream gene
23	chr8:27652201-27652500	9	ENSGALG00000011238	WLS	upstream gene
			ENSGALG00000027802	gga-mir-6653	downstream gene
24	chr8:28043701-28044000	3	--	Intergenic region (8)	intergenic
25	chr10:2100301-2100600	27	ENSGALG00000001449	STRA6	downstream gene
			ENSGALG00000021525	ISLR	coding sequence ; regulatory region
			ENSGALG00000029151	Novel gene (4)	downstream gene
26	chr10:12681001-12681600	5	--	Intergenic region (9)	intergenic
27	chr10:19580401-19581000	43	ENSGALG00000008315	UNC45A	upstream gene
			ENSGALG00000008336	MAN2A2	coding sequence ; intronic ; regulatory region
28	chr10:19592401-19593000	21	ENSGALG00000008340	FES	intronic ; regulatory region
			ENSGALG00000008341	FURIN	downstream gene
29	chr11:453601-453900	29	ENSGALG00000000904	USB1	upstream gene
			ENSGALG00000000999	ZNF319	coding sequence ; regulatory region
			ENSGALG00000001011	CNGB1	upstream gene
			ENSGALG00000000904	USB1	upstream gene
30	chr11:17139901-17140500	26	ENSGALG00000014284	GSE1	intronic ; regulatory region
31	chr11:19161901-19162200	8	ENSGALG00000000802	DHODH	downstream gene
			ENSGALG00000000811	IST1	downstream gene
			ENSGALG00000000787	DHX38	upstream gene

32	chr12:3190201-3190500	11	ENSGALG00000004639	GNAI2	downstream gene
			ENSGALG00000013370	SEMA3F	downstream gene
			ENSGALG00000028697	GNAT1	coding sequence ; intronic ; regulatory region
33	chr12:5752201-5752800	12	--	Intergenic region (10)	intergenic
34	chr12:11534101-11534700	23	--	Intergenic region (11)	intergenic
35	chr13:15793201-15793800	9	ENSGALG00000006569	Novel gene (5)	downstream gene
36	chr15:2566201-2566500	6	ENSGALG00000002272	NOC4L	coding sequence ; intronic ; regulatory region
			ENSGALG00000002336	RP11-2C24.9	downstream gene
37	chr15:7104601-7104900	5	--	Intergenic region (12)	intergenic
38	chr15:9882901-9883200	6	ENSGALG00000007396	TAOK3	coding sequence ; intronic ; regulatory region
39	chr15:10068901-10069200	24	ENSGALG00000007720	AIFM3	downstream gene
			ENSGALG00000028023	C14ORF166B	start lost; coding sequence ; 5 prime UTR
			ENSGALG00000026902	P2RX6	coding sequence ; intronic ; regulatory region
40	chr15:10800301-10800600	6	ENSGALG00000007781	GAL3ST1	downstream gene
			ENSGALG00000007840	RP4-539M6.19	downstream gene
41	chr16:70501-71100	13	ENSGALG00000000178	BF1	downstream gene
			ENSGALG00000000181	Novel gene (6)	upstream gene
			ENSGALG00000026269	TAP1	coding sequence ; intronic ; regulatory region
42	chr16:219901-220500	11	ENSGALG00000019836	ZNF692	coding sequence ; intronic ; regulatory region
			ENSGALG00000028962	Novel gene (7)	upstream gene
43	chr17:168901-169200	1	--	Intergenic region (13)	intergenic
			ENSGALG00000019837	KIFC1	downstream gene
			ENSGALG00000028962	Novel gene (7)	upstream gene
44	chr17:8289901-8290500	28	ENSGALG00000001595	PHF19	coding sequence ; intronic ; regulatory region
			ENSGALG00000001620	CUTA	downstream gene
45	chr17:8550001-8550600	24	ENSGALG00000001419	DAB2IP	intronic ; regulatory region
46	chr17:9845701-9846000	10	--	Intergenic region (14)	intergenic
47	chr19:4471201-4471800	12	ENSGALG00000002186	UNC45B	coding sequence ; intronic ; regulatory region
			ENSGALG00000002212	RAD51D	upstream gene
48	chr19:4753501-4754100	22	ENSGALG00000002312	TMEM132E	coding sequence ; intronic ; regulatory region
49	chr19:8303401-8304000	11	--	Intergenic region (15)	intergenic
50	chr20:2325901-2326500	13	--	Intergenic region (16)	intergenic
51	chr20:8868601-8868900	37	--	Intergenic region (17)	intergenic
52	chr20:9458401-9458700	2	ENSGALG00000005932	MYT1	coding sequence ; intronic ; regulatory region
53	chr20:11843101-11843700	31	ENSGALG00000007636	PCK1	intronic ; regulatory region
54	chr20:11844601-11845200	17	ENSGALG00000007636	PCK1	intronic ; regulatory region
55	chr21:4398301-4398600	12	ENSGALG00000027085	CROCC	coding sequence ; intronic ; regulatory region
56	chr22:1246501-1247100	19	ENSGALG00000000402	LOXL2	downstream gene
			ENSGALG00000000405	R3HCC1	coding sequence ; intronic ; regulatory region
57	chr24:2467801-2468100	10	ENSGALG00000001450	IGSF9B	upstream gene
58	chr25:15301-15900	37	ENSGALG00000009011	SMG5	upstream gene
59	chr25:209701-210300	34	ENSGALG00000000443	Novel gene (8)	intronic ; regulatory region
60	chr25:225301-225900	21	--	Intergenic region (18)	intergenic
61	chr25:234901-235500	20	--	Intergenic region (19)	intergenic
62	chr25:243301-243600	12	--	Intergenic region (20)	intergenic
63	chr25:660001-660300	17	ENSGALG00000027046	Novel gene (9)	coding sequence ; intronic ; regulatory region
64	chr25:1675201-1675800	54	ENSGALG00000022137	CRP	coding sequence ; regulatory region
			ENSGALG00000028854	DUSP23	upstream gene
65	chr26:648601-648900	6	ENSGALG00000000362	NAV1	coding sequence ; intronic ; regulatory region
			ENSGALG00000028854	DUSP23	upstream gene
			ENSGALG00000027054	Novel gene (10)	downstream gene
			ENSGALG00000028795	CADM3	downstream gene
66	chr26:1633201-1633800	12	ENSGALG00000000583	SOX13	intronic ; regulatory region

67	chr26:1707301-1707600	5	ENSGALG00000000587	PLEKHA6	intronic ; regulatory region
68	chr26:4467901-4468200	8	--	Intergenic region (21)	intergenic
69	chr27:2586001-2586300	5	ENSGALG00000000478	TANC2	intronic ; regulatory region
70	chr27:4113601-4113900	12	ENSGALG00000025788	CACNB1	coding sequence ; intronic ; regulatory region
71	chr28:2780701-2781300	25	ENSGALG00000026231	ARID3A	intronic ; regulatory region
72	chr28:3127801-3128100	8	ENSGALG00000024298	ADAMTSL5	downstream gene
			ENSGALG00000026384	PCSK4	downstream gene
73	chrZ:1446301-1446900	16	--	Intergenic region (22)	intergenic
74	chrZ:56827201-56827800	76	ENSGALG00000014684	ERAP1	upstream gene

Supplementary Table 3
Results for Consensus PathDB network analyses

1) Pathway over-representation analysis

47 genes (68.1%) from the input list are present in at least one pathway

pathway name	pathway source	set size	candidates contained	p-value	q-value
G-protein activation	Reactome	28	3 (10.7%)	0.00021	0.0323
Activation of the phototransduction cascade	Reactome	11	2 (18.2%)	0.00093	0.0708
cell cycle: g2/m checkpoint	BioCarta	21	2 (9.5%)	0.00344	0.0899
ADP signalling through P2Y purinoceptor 12	Reactome	22	2 (9.1%)	0.00378	0.0899
Adrenaline,noradrenaline inhibits insulin secretion	Reactome	23	2 (8.7%)	0.00413	0.0899
MAPK signaling pathway - Homo sapiens (human)	KEGG	257	5 (2.0%)	0.00414	0.0899
Visual signal transduction: Rods	PID	24	2 (8.3%)	0.00449	0.0899
Opioid Signalling	Reactome	84	3 (3.6%)	0.00504	0.0899
p38 MAPK signaling pathway	PID	29	2 (6.9%)	0.00652	0.0899
Phototransduction - Homo sapiens (human)	KEGG	29	2 (6.9%)	0.00652	0.0899
Signal amplification	Reactome	31	2 (6.5%)	0.00742	0.0899
Visual phototransduction	Reactome	96	3 (3.1%)	0.00754	0.0899
Inactivation, recovery and regulation of the phototransduction cascade	Reactome	32	2 (6.2%)	0.0079	0.0899
The phototransduction cascade	Reactome	33	2 (6.1%)	0.00838	0.0899
mRNA 3,-end processing	Reactome	35	2 (5.7%)	0.0094	0.0899
Post-Elongation Processing of Intron-Containing pre-mRNA	Reactome	35	2 (5.7%)	0.0094	0.0899

2) Enriched gene ontology (GO) terms

67 genes (97.1%) from the input list are present in at least one GO category

gene ontology term		category, level	set size	candidates contained	p-value	q-value
GO:0019885	antigen processing and presentation of endogenous peptide antigen via MHC class I	BP 5	11	2 (18.2%)	0.00068	0.0936
GO:0001578	microtubule bundle formation	BP 5	67	3 (4.5%)	0.0018	0.123
GO:0019001	guanyl nucleotide binding	MF 5	394	6 (1.5%)	0.00276	0.0412
GO:0032550	purine ribonucleoside binding	MF 5	1828	14 (0.8%)	0.00458	0.0412
GO:0051297	centrosome organization	BP 5	97	3 (3.1%)	0.00512	0.234
GO:0007602	phototransduction	BP 5	115	3 (2.6%)	0.00819	0.26
GO:0042461	photoreceptor cell development	BP 5	41	2 (4.9%)	0.0095	0.26

Fig. S1. Relation between Individual average coverage (S.Cov) and percentage of the genome covered (%Cov). The size of the balloons represent the cut-off index defined as %Cov/S.Cov * 100.

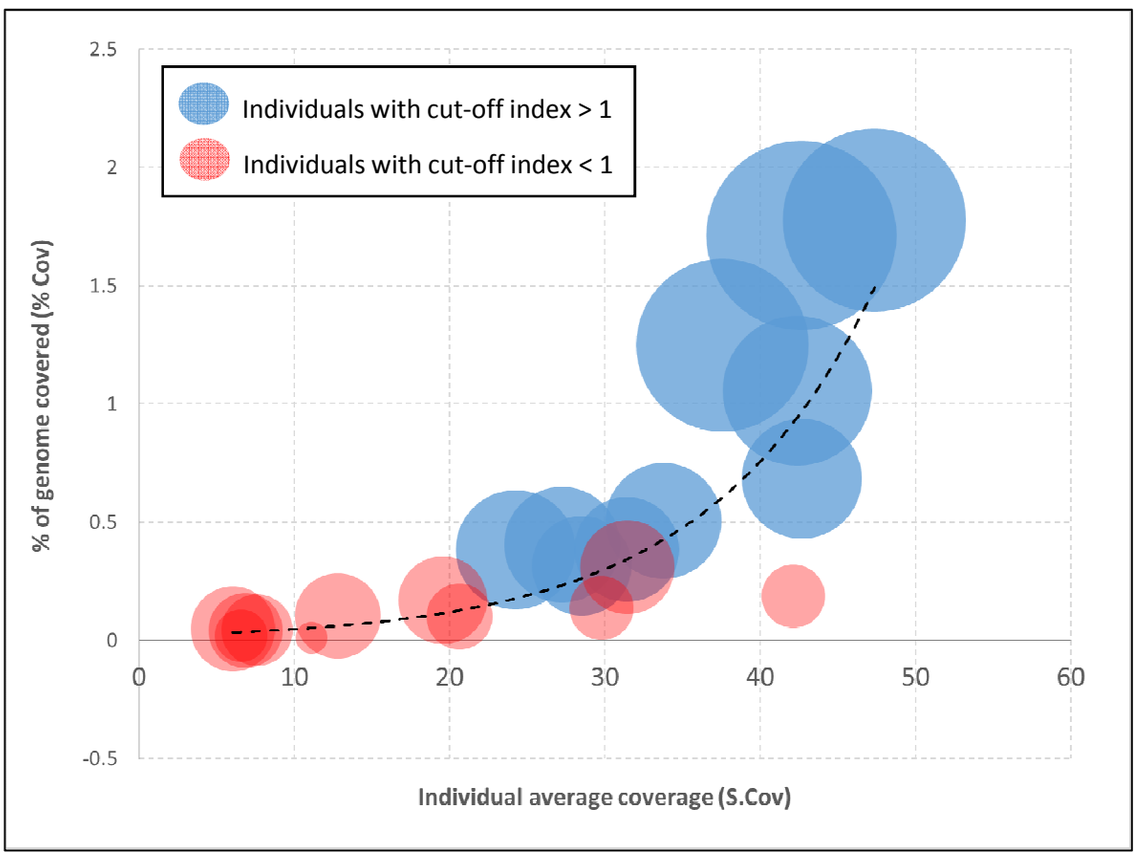

	Coverage	Number of bases covered	Unique nucleotides sequenced	% of the Chicken Genome Covered	Cut-off index	Passed cut-off index?
RJF_AV163_cleaned_sorted.bam	42.65	785050701	18407679	1.71	4.02	Y
RJF_C165_cleaned_sorted.bam	47.36	904820256	19107134	1.78	3.75	Y
RJF_C167_cleaned_sorted.bam	37.56	503891013	13415736	1.25	3.32	Y
RJF_AV171_cleaned_sorted.bam	42.39	481170980	11350889	1.06	2.49	Y
RJF_C175_cleaned_sorted.bam	42.69	313281350	7337848	0.68	1.60	Y
RJF_AV170_cleaned_sorted.bam	24.25	100141920	4129700	0.38	1.58	Y
RJF_C172_cleaned_sorted.bam	33.79	183302789	5424893	0.50	1.49	Y
RJF_AV176_cleaned_sorted.bam	27.24	118755610	4359012	0.41	1.49	Y
RJF_C174_cleaned_sorted.bam	31.39	129808223	4135284	0.38	1.23	Y
RJF_C178_cleaned_sorted.bam	28.51	96777429	3394282	0.32	1.11	Y
RJF_C164_cleaned_sorted.bam	31.43	104579349	3327659	0.31	0.99	N
RJF_C181_cleaned_sorted.bam	19.55	35561207	1819164	0.17	0.87	N
RJF_C182_cleaned_sorted.bam	12.80	14262264	1114109	0.10	0.81	N
RJF_C180_cleaned_sorted.bam	6.04	3134870	519214	0.05	0.80	N
RJF_C184_cleaned_sorted.bam	6.85	3145741	458998	0.04	0.62	N
RJF_AV179_cleaned_sorted.bam	7.60	3560878	468367	0.04	0.57	N
RJF_AV186_cleaned_sorted.bam	20.64	22434655	1086845	0.10	0.49	N
RJF_C173_cleaned_sorted.bam	29.78	43589534	1463841	0.14	0.46	N
RJF_AV177_cleaned_sorted.bam	42.13	84819706	2013414	0.19	0.44	N
RJF_AV166_cleaned_sorted.bam	6.57	1426214	217137	0.02	0.31	N
RJF_AV169_cleaned_sorted.bam	11.12	1505151	135301	0.01	0.11	N
Average	**26.30200667**	**187381897.1**	**4937452.683**	**0.45931501**	**1.36**	

Fig. S2. A) Network analysis performed with Consensus PathDB showing how the DMR associated genes relate to biological pathways and gene ontology information. Significantly enriched pathways and GO terms are shown. Significance values for the pathway over-representation analysis and enriched GO terms are shown in Supplementary Table 3. The numbers within circles correspond to DMR-associated genes within a specific affected biological pathway (circles with blue annotations) or GO terms (circles with pink annotations). The size of the circles correspond to the total number of genes in the database for that specific pathway. **B)** and **C)** Network analysis performed with Reactome showing how the DMR associated genes relate to biological pathways. Significantly enriched pathways are shown for the immune system **(B)** and signal transduction **(C)**.

A)

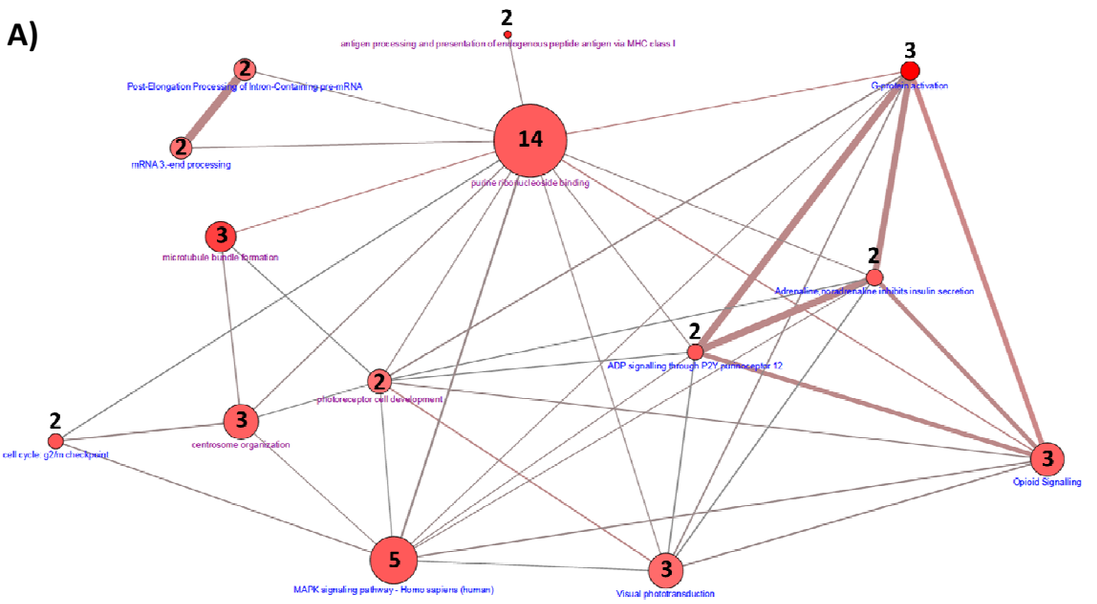

B)

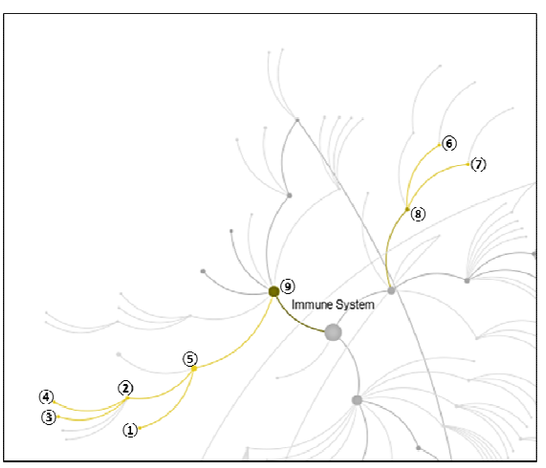

1- Antigen Presentation: Folding, assembly and peptide loading of class I MHC
2- Antigen processing-Cross presentation
3- ER-Phagosome pathway
4- Endosomal/Vacuolar pathway
5- Class I MHC mediated antigen processing & presentation
6- Interferon alpha/beta signaling
7- Interferon gamma signaling
8- Interferon Signaling
9- Adaptive Immune System

C)

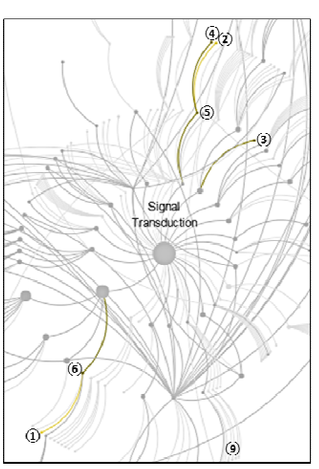

1- G-protein activation
2- Activation of the phototransduction cascade
3- Nerve growth factor (NGF) processing
4- Inactivation, recovery and regulation of the phototransduction cascade
5- The phototransduction cascade
6- Opioid Signaling

Table S1

	Location	Gene	SYMBOL	edgeR logFC	edgeR logCPM	edgeR p-value	edgeR adj p-value
1	chr1:1244701-1245000	ENSGALG00000008449	novel gene	4.448	3.344	0.005	4.69E-03
2	chr1:1245001-1245300			4.448	3.344	0.005	4.69E-03
3	chr1:44775901-44776200	ENSGALG00000011297	CRADD	-1.373	6.134	0.003	2.79E-03
4	chr1:81671101-81671400	-	-	2.877	4.270	0.002	1.77E-03
5	chr1:81671401-81671700			2.877	4.270	0.002	1.77E-03
6	chr1:143647201-143647500	-	-	2.179	4.363	0.002	2.32E-03
7	chr1:143647501-143647800			2.179	4.363	0.002	2.32E-03
8	chr1:193971001-193971300	ENSGALG00000009114	DGAT2	2.541	3.400	0.004	4.08E-03
9	chr1:193971301-193971600			2.541	3.400	0.004	4.08E-03
10	chr1:193971601-193971900			3.195	3.370	0.004	3.73E-03
11	chr2:223501-223800	ENSGALG00000013341	AGAP3	3.053	3.326	0.003	2.74E-03
12	chr2:112513801-112514100	ENSGALG00000015450	RAB2A	-3.924	4.005	0.003	3.37E-03
13	chr4:13297201-13297500	ENSGALG00000008006	CAPN6	2.767	3.510	0.003	3.14E-03
14	chr4:13429201-13429500	-	-	-1.567	4.940	0.003	2.67E-03
15	chr4:34189801-34190100	ENSGALG00000010291 ENSGALG00000010298	RBPMS; DCTN6	2.286	4.055	0.003	3.36E-03
16	chr4:34190101-34190400			2.557	3.982	0.003	2.71E-03
17	chr4:44742601-44742900	ENSGALG00000010893	FGF5	-2.695	4.638	0.000	2.65E-04
18	chr5:402001-402300	ENSGALG00000013298	CPSF7	3.572	3.779	0.002	1.88E-03
		ENSGALG00000022369	TMEM216				
		ENSGALG00000025756	TMEM138				
19	chr5:5731501-5731800	-	-	-0.713	8.232	0.003	3.36E-03
20	chr5:5731801-5732100			-0.712	8.514	0.002	1.82E-03
21	chr5:43370101-43370400	ENSGALG00000010680	TTC7B	3.802	3.585	0.000	4.92E-04
22	chr5:43370401-43370700			3.802	3.585	0.000	4.92E-04
23	chr5:56258101-56258400	ENSGALG00000012203	SAMD4A	-1.651	5.633	0.001	1.43E-03
24	chr5:56258401-56258700			-1.651	5.633	0.001	1.43E-03
25	chr5:57753301-57753600	ENSGALG00000012321	MAP4K5	-5.357	4.037	0.001	5.13E-04
26	chr5:57753601-57753900			-5.385	4.055	0.000	4.59E-04
27	chr6:27634201-27634500	ENSGALG00000025403	MIR1815	3.831	3.561	0.003	2.92E-03
28	chr6:27634501-27634800			3.831	3.561	0.003	2.92E-03
29	chr7:10155301-10155600	-	-	3.461	3.442	0.002	2.22E-03
30	chr7:10155601-10155900			3.461	3.442	0.002	2.22E-03
31	chr7:34455901-34456200	-	-	3.254	3.374	0.001	1.40E-03
32	chr7:34456201-34456500			3.254	3.374	0.001	1.40E-03
33	chr7:34456501-34456800	ENSGALG00000012475	novel gene	3.494	3.455	0.001	1.38E-03
34	chr8:3895201-3895500	-	-	2.440	3.704	0.002	1.61E-03
		ENSGALG00000010226	MUTYH				

35	chr8:19935901-19936200	ENSGALG00000010228	TOE1	1.891	4.176	0.005	4.58E-03
		ENSGALG00000023348	HPDL				
36	chr8:27597601-27597900	ENSGALG00000026591	GNG12	-1.819	4.950	0.002	2.49E-03
		ENSGALG00000025977	GADD45A				
37	chr8:27652201-27652500	ENSGALG00000011238	WLS	4.908	3.584	0.004	3.80E-03
		ENSGALG00000027802	gga-mir-6653				
38	chr8:28043701-28044000	-	-	-2.832	4.513	0.003	3.01E-03
39	chr10:2100301-2100600	ENSGALG00000001449	STRA6	-2.742	4.917	0.004	4.00E-03
		ENSGALG00000021525	ISLR				
		ENSGALG00000029151	novel gene				
40	chr10:12681001-12681300	-	-	4.800	3.523	0.004	3.92E-03
41	chr10:12681301-12681600	-	-	4.616	3.435	0.005	4.78E-03
42	chr10:19580401-19580700	ENSGALG00000008315 ENSGALG00000008336	UNC45A; MAN2A2	1.612	5.653	0.000	2.52E-04
43	chr10:19580701-19581000			1.708	5.559	0.000	1.90E-04
44	chr10:19592401-19592700	ENSGALG00000008340 ENSGALG00000008341	FES; FURIN	3.584	3.748	0.002	1.99E-03
45	chr10:19592701-19593000			3.584	3.748	0.002	1.99E-03
46	chr11:453601-453900	ENSGALG00000000904	USB1	3.478	3.400	0.004	4.02E-03
		ENSGALG00000000999	ZNF319				
		ENSGALG00000001011	CNGB1				
47	chr11:17139901-17140200	ENSGALG00000014284	GSE1	-5.359	4.016	0.003	3.01E-03
48	chr11:17140201-17140500			-5.359	4.016	0.003	3.01E-03
49	chr11:19161901-19162200	ENSGALG00000000802	DHODH	3.019	3.598	0.002	1.81E-03
		ENSGALG00000000811	IST1				
		ENSGALG00000000787	DHX38				
50	chr12:3190201-3190500	ENSGALG00000004639	GNAI2	2.362	4.114	0.005	4.95E-03
		ENSGALG00000013370	SEMA3F				
		ENSGALG00000028697	GNAT1				
51	chr12:5752201-5752500	-	-	-2.520	4.337	0.004	4.40E-03
52	chr12:5752501-5752800			-2.549	4.034	0.001	7.62E-04
53	chr12:11534101-11534400	-	-	-1.405	5.706	0.003	3.14E-03
54	chr12:11534401-11534700			-1.338	5.596	0.004	3.93E-03
55	chr13:15793201-15793500	ENSGALG00000006569	novel gene	2.434	4.351	0.005	4.97E-03

56	chr13:15793501-15793800	ENSGALG00000006569	novel gene	2.551	4.488	0.002	1.99E-03
57	chr15:2566201-2566500	ENSGALG00000002272	NOC4L	4.472	3.349	0.003	3.14E-03
		ENSGALG00000002336	RP11-2C24.9				
58	chr15:7104601-7104900	-	-	-3.205	4.148	0.004	3.67E-03
59	chr15:9882901-9883200	ENSGALG00000007396	TAOK3	2.858	3.697	0.001	9.83E-04
60	chr15:10068901-10069200	ENSGALG00000007720	AIFM3	1.460	4.850	0.004	4.38E-03
		ENSGALG00000028023	C14ORF166B				
		ENSGALG00000026902	P2RX6				
61	chr15:10800301-10800600	ENSGALG00000007781	GAL3ST1	-1.368	5.310	0.004	4.14E-03
		ENSGALG00000007840	RP4-539M6.19				
62	chr16:70501-70800	ENSGALG00000000178 ENSGALG00000000181 ENSGALG00000026269	BF1; novel gene; TAP1	2.832	4.523	0.001	8.84E-04
63	chr16:70801-71100			2.832	4.523	0.001	8.84E-04
64	chr16:219901-220200	ENSGALG00000019836 ENSGALG00000028962	ZNF692 novelgene	-5.336	4.053	0.003	2.77E-03
65	chr16:220201-220500			-5.393	4.088	0.002	2.42E-03
66	chr17:168901-169200	ENSGALG00000019837	KIFC1	1.344	4.824	0.005	4.74E-03
67	chr17:8289901-8290200	ENSGALG00000001595 ENSGALG00000001620	PHF19; CUTA	-3.805	5.124	0.001	8.25E-04
68	chr17:8290201-8290500			-3.677	3.935	0.001	1.25E-03
69	chr17:8550001-8550300	ENSGALG00000001419	DAB2IP	2.939	4.030	0.004	3.58E-03
70	chr17:8550301-8550600			2.939	4.030	0.004	3.58E-03
71	chr17:9845701-9846000	-	-	-5.019	3.840	0.002	1.58E-03
72	chr19:4471201-4471500	ENSGALG00000002186 ENSGALG00000002212	UNC45B; RAD51D	2.321	3.861	0.002	2.13E-03
73	chr19:4471501-4471800			2.321	3.861	0.002	2.13E-03
74	chr19:4753501-4753800	ENSGALG00000002312	TMEM132E	1.650	4.849	0.003	2.50E-03
75	chr19:4753801-4754100			1.669	4.859	0.003	2.59E-03
76	chr19:8303401-8303700	-	-	4.901	3.525	0.001	9.14E-04
77	chr19:8303701-8304000			4.901	3.525	0.001	9.14E-04
78	chr20:2325901-2326200	-	-	-4.852	4.715	0.001	7.05E-04
79	chr20:2326201-2326500			-4.115	4.730	0.003	2.62E-03
80	chr20:8868601-8868900	-	-	3.123	3.889	0.000	4.05E-04
81	chr20:9458401-9458700	ENSGALG00000005932	MYT1	-3.928	4.105	0.005	4.53E-03
82	chr20:11843101-11843400	ENSGALG00000007636	PCK1	-2.591	4.055	0.001	1.37E-03
83	chr20:11843401-11843700			-2.453	3.975	0.002	2.27E-03
84	chr20:11844601-11844900			-2.149	4.166	0.003	2.82E-03
85	chr20:11844901-11845200			-2.149	4.166	0.003	2.82E-03

86	chr21:4398301-4398600	ENSGALG00000027085	CROCC	1.579	5.808	0.000	4.36E-04
87	chr22:1246501-1246800	ENSGALG00000000402	LOXL2	-1.682	5.492	0.002	1.87E-03
		ENSGALG00000000405	R3HCC1				
88	chr22:1246801-1247100			-1.724	5.320	0.003	2.83E-03
89	chr24:2467801-2468100	ENSGALG00000001450	IGSF9B	3.291	3.378	0.004	3.57E-03
90	chr25:15301-15600	ENSGALG00000009011	SMG5	1.640	4.771	0.004	3.87E-03
91	chr25:15601-15900			1.640	4.771	0.004	3.87E-03
92	chr25:209701-210000	ENSGALG00000000443	novel gene	1.467	7.140	0.001	1.06E-03
93	chr25:210001-210300			1.954	6.799	0.000	3.49E-05
94	chr25:225301-225600	-	-	2.562	5.493	0.002	2.38E-03
95	chr25:225601-225900			2.420	5.586	0.002	1.78E-03
96	chr25:234901-235200	-	-	2.406	5.405	0.004	4.09E-03
97	chr25:235201-235500			2.394	5.426	0.004	3.86E-03
98	chr25:243301-243600	-	-	1.441	6.808	0.001	5.96E-04
99	chr25:660001-660300	ENSGALG00000027046	novel gene	3.421	3.810	0.005	4.91E-03
100	chr25:1675201-1675500	ENSGALG00000028854	DUSP23	1.213	5.974	0.004	4.41E-03
		ENSGALG00000022137	CRP				
101	chr25:1675501-1675800	ENSGALG00000027054 ENSGALG0000002879	novel gene; CADM3	1.213	5.974	0.004	4.41E-03
102	chr26:648601-648900	ENSGALG00000000362	NAV1	-1.825	4.777	0.005	4.69E-03
		ENSGALG00000028854	DUSP23				
103	chr26:1633201-1633500	ENSGALG00000000583	SOX13	3.188	3.594	0.002	2.18E-03
104	chr26:1633501-1633800			3.188	3.594	0.002	2.18E-03
105	chr26:1707301-1707600	ENSGALG00000000587	PLEKHA6	1.772	4.710	0.002	1.77E-03
106	chr26:4467901-4468200	-	-	-3.344	3.754	0.004	4.25E-03
107	chr27:2586001-2586300	ENSGALG00000000478	TANC2	3.125	3.321	0.005	4.69E-03
108	chr27:4113601-4113900	ENSGALG00000025788	CACNB1	3.252	3.461	0.004	4.33E-03
109	chr28:2780701-2781000	ENSGALG00000026231	ARID3A	-5.524	4.143	0.001	1.14E-03
110	chr28:2781001-2781300			-5.524	4.143	0.001	1.14E-03
111	chr28:3127801-3128100	ENSGALG00000024298	ADAMTSL5	2.225	3.991	0.003	3.27E-03
		ENSGALG00000026384	PCSK4				
112	chrZ:1446301-1446600	-	-	3.788	3.612	0.003	2.86E-03
123	chrZ:1446601-1446900			3.707	3.576	0.004	3.74E-03
114	chrZ:56827201-56827500	ENSGALG00000014684	ERAP1	1.661	4.443	0.003	2.79E-03
115	chrZ:56827501-56827800			1.661	4.443	0.003	2.79E-03

Table S2

Merged windows with differential methylation		CpGs within the merged window	DMR within or near gene		Position regarding gene
			ENSEMBL name	Gene symbol	
1	chr1:1244701-1245300	5	ENSGALG00000008449	Novel gene (1)	coding sequence ; intronic ; regulatory region
2	chr1:44775901-44776200	12	ENSGALG00000011297	CRADD	intronic ; regulatory region
3	chr1:81671101-81671700	10	--	Intergenic region (1)	intergenic
4	chr1:143647201-143647800	29	--	Intergenic region (2)	intergenic
5	chr1:193971001-193971900	36	ENSGALG00000009114	DGAT2	upstream gene
6	chr2:223501-223800	19	ENSGALG00000013341	AGAP3	intronic ; regulatory region
7	chr2:112513801-112514100	6	ENSGALG00000015450	RAB2A	upstream gene
8	chr4:13297201-13297500	4	ENSGALG00000008006	CAPN6	intronic ; regulatory region
9	chr4:13429201-13429500	11	--	Intergenic region (3)	intergenic
			ENSGALG00000010298	DCTN6	downstream gene
10	chr4:34189801-34190400	20	ENSGALG00000010291	RBPMS	coding sequence ; intronic ; regulatory region
11	chr4:44742601-44742900	14	ENSGALG00000010893	FGF5	coding sequence ; intronic ; regulatory region
12	chr5:402001-402300	10	ENSGALG00000013298	CPSF7	downstream gene
			ENSGALG00000022369	TMEM216	upstream gene
			ENSGALG00000025756	TMEM138	coding sequence ; intronic ; regulatory region
			ENSGALG00000028882	Novel gene (2)	upstream gene
13	chr5:5731501-5732100	29	--	Intergenic region (4)	intergenic
14	chr5:43370101-43370700	10	ENSGALG00000010680	TTC7B	intronic ; regulatory region
15	chr5:56258101-56258700	34	ENSGALG00000012203	SAMD4A	intronic ; regulatory region
16	chr5:57753301-57753900	6	ENSGALG00000012321	MAP4K5	upstream gene
17	chr6:27634201-27634800	3	ENSGALG00000025403	MIR1815	upstream gene
18	chr7:10155301-10155900	13	--	Intergenic region (5)	intergenic
19	chr7:34455901-34456800	20	--	Intergenic region (6)	intergenic
			ENSGALG00000012475	Novel gene (3)	downstream gene
20	chr8:3895201-3895500	7	--	Intergenic region (7)	intergenic
21	chr8:19935901-19936200	3	ENSGALG00000010226	MUTYH	coding sequence ; intronic ; regulatory region
			ENSGALG00000010228	TOE1	upstream gene
			ENSGALG00000023348	HPDL	downstream gene
22	chr8:27597601-27597900	8	ENSGALG00000026591	GNG12	coding sequence ; intronic ; regulatory region
			ENSGALG00000025977	GADD45A	downstream gene
23	chr8:27652201-27652500	9	ENSGALG00000011238	WLS	upstream gene
			ENSGALG00000027802	gga-mir-6653	downstream gene
24	chr8:28043701-28044000	3	--	Intergenic region (8)	intergenic
25	chr10:2100301-2100600	27	ENSGALG00000001449	STRA6	downstream gene
			ENSGALG00000021525	ISLR	coding sequence ; regulatory region
			ENSGALG00000029151	Novel gene (4)	downstream gene
26	chr10:12681001-12681600	5	--	Intergenic region (9)	intergenic
27	chr10:19580401-19581000	43	ENSGALG00000008315	UNC45A	upstream gene
			ENSGALG00000008336	MAN2A2	coding sequence ; intronic ; regulatory region
28	chr10:19592401-19593000	21	ENSGALG00000008340	FES	intronic ; regulatory region
			ENSGALG00000008341	FURIN	downstream gene
29	chr11:453601-453900	29	ENSGALG00000000904	USB1	upstream gene
			ENSGALG00000000999	ZNF319	coding sequence ; regulatory region
			ENSGALG00000001011	CNGB1	upstream gene
			ENSGALG00000000904	USB1	upstream gene
30	chr11:17139901-17140500	26	ENSGALG00000014284	GSE1	intronic ; regulatory region
31	chr11:19161901-19162200	8	ENSGALG00000000802	DHODH	downstream gene
			ENSGALG00000000811	IST1	downstream gene
			ENSGALG00000000787	DHX38	upstream gene

32	chr12:3190201-3190500	11	ENSGALG00000004639	GNAI2	downstream gene
			ENSGALG00000013370	SEMA3F	downstream gene
			ENSGALG00000028697	GNAT1	coding sequence ; intronic ; regulatory region
33	chr12:5752201-5752800	12	--	Intergenic region (10)	intergenic
34	chr12:11534101-11534700	23	--	Intergenic region (11)	intergenic
35	chr13:15793201-15793800	9	ENSGALG00000006569	Novel gene (5)	downstream gene
36	chr15:2566201-2566500	6	ENSGALG00000002272	NOC4L	coding sequence ; intronic ; regulatory region
			ENSGALG00000002336	RP11-2C24.9	downstream gene
37	chr15:7104601-7104900	5	--	Intergenic region (12)	intergenic
38	chr15:9882901-9883200	6	ENSGALG00000007396	TAOK3	coding sequence ; intronic ; regulatory region
39	chr15:10068901-10069200	24	ENSGALG00000007720	AIFM3	downstream gene
			ENSGALG00000028023	C14ORF166B	start lost; coding sequence ; 5 prime UTR
			ENSGALG00000026902	P2RX6	coding sequence ; intronic ; regulatory region
40	chr15:10800301-10800600	6	ENSGALG00000007781	GAL3ST1	downstream gene
			ENSGALG00000007840	RP4-539M6.19	downstream gene
41	chr16:70501-71100	13	ENSGALG00000000178	BF1	downstream gene
			ENSGALG00000000181	Novel gene (6)	upstream gene
			ENSGALG00000026269	TAP1	coding sequence ; intronic ; regulatory region
42	chr16:219901-220500	11	ENSGALG00000019836	ZNF692	coding sequence ; intronic ; regulatory region
			ENSGALG00000028962	Novel gene (7)	upstream gene
43	chr17:168901-169200	1	--	Intergenic region (13)	intergenic
			ENSGALG00000019837	KIFC1	downstream gene
			ENSGALG00000028962	Novel gene (7)	upstream gene
44	chr17:8289901-8290500	28	ENSGALG00000001595	PHF19	coding sequence ; intronic ; regulatory region
			ENSGALG00000001620	CUTA	downstream gene
45	chr17:8550001-8550600	24	ENSGALG00000001419	DAB2IP	intronic ; regulatory region
46	chr17:9845701-9846000	10	--	Intergenic region (14)	intergenic
47	chr19:4471201-4471800	12	ENSGALG00000002186	UNC45B	coding sequence ; intronic ; regulatory region
			ENSGALG00000002212	RAD51D	upstream gene
48	chr19:4753501-4754100	22	ENSGALG00000002312	TMEM132E	coding sequence ; intronic ; regulatory region
49	chr19:8303401-8304000	11	--	Intergenic region (15)	intergenic
50	chr20:2325901-2326500	13	--	Intergenic region (16)	intergenic
51	chr20:8868601-8868900	37	--	Intergenic region (17)	intergenic
52	chr20:9458401-9458700	2	ENSGALG00000005932	MYT1	coding sequence ; intronic ; regulatory region
53	chr20:11843101-11843700	31	ENSGALG00000007636	PCK1	intronic ; regulatory region
54	chr20:11844601-11845200	17	ENSGALG00000007636	PCK1	intronic ; regulatory region
55	chr21:4398301-4398600	12	ENSGALG00000027085	CROCC	coding sequence ; intronic ; regulatory region
56	chr22:1246501-1247100	19	ENSGALG00000000402	LOXL2	downstream gene
			ENSGALG00000000405	R3HCC1	coding sequence ; intronic ; regulatory region
57	chr24:2467801-2468100	10	ENSGALG00000001450	IGSF9B	upstream gene
58	chr25:15301-15900	37	ENSGALG00000009011	SMG5	upstream gene
59	chr25:209701-210300	34	ENSGALG00000000443	Novel gene (8)	intronic ; regulatory region
60	chr25:225301-225900	21	--	Intergenic region (18)	intergenic
61	chr25:234901-235500	20	--	Intergenic region (19)	intergenic
62	chr25:243301-243600	12	--	Intergenic region (20)	intergenic
63	chr25:660001-660300	17	ENSGALG00000027046	Novel gene (9)	coding sequence ; intronic ; regulatory region
64	chr25:1675201-1675800	54	ENSGALG00000022137	CRP	coding sequence ; regulatory region
			ENSGALG00000028854	DUSP23	upstream gene
65	chr26:648601-648900	6	ENSGALG00000000362	NAV1	coding sequence ; intronic ; regulatory region
			ENSGALG00000028854	DUSP23	upstream gene
			ENSGALG00000027054	Novel gene (10)	downstream gene
			ENSGALG00000028795	CADM3	downstream gene
66	chr26:1633201-1633800	12	ENSGALG00000000583	SOX13	intronic ; regulatory region

67	chr26:1707301-1707600	5	ENSGALG00000000587	PLEKHA6	intronic ; regulatory region
68	chr26:4467901-4468200	8	--	Intergenic region (21)	intergenic
69	chr27:2586001-2586300	5	ENSGALG00000000478	TANC2	intronic ; regulatory region
70	chr27:4113601-4113900	12	ENSGALG00000025788	CACNB1	coding sequence ; intronic ; regulatory region
71	chr28:2780701-2781300	25	ENSGALG00000026231	ARID3A	intronic ; regulatory region
72	chr28:3127801-3128100	8	ENSGALG00000024298	ADAMTSL5	downstream gene
			ENSGALG00000026384	PCSK4	downstream gene
73	chrZ:1446301-1446900	16	--	Intergenic region (22)	intergenic
74	chrZ:56827201-56827800	76	ENSGALG00000014684	ERAP1	upstream gene

Table S3
Results for Consensus PathDB network analyses

1) Pathway over-representation analysis

47 genes (68.1%) from the input list are present in at least one pathway

pathway name	pathway source	set size	candidates contained	p-value	q-value
G-protein activation	Reactome	28	3 (10.7%)	0.00021	0.0323
Activation of the phototransduction cascade	Reactome	11	2 (18.2%)	0.00093	0.0708
cell cycle: g2/m checkpoint	BioCarta	21	2 (9.5%)	0.00344	0.0899
ADP signalling through P2Y purinoceptor 12	Reactome	22	2 (9.1%)	0.00378	0.0899
Adrenaline,noradrenaline inhibits insulin secretion	Reactome	23	2 (8.7%)	0.00413	0.0899
MAPK signaling pathway - Homo sapiens (human)	KEGG	257	5 (2.0%)	0.00414	0.0899
Visual signal transduction: Rods	PID	24	2 (8.3%)	0.00449	0.0899
Opioid Signalling	Reactome	84	3 (3.6%)	0.00504	0.0899
p38 MAPK signaling pathway	PID	29	2 (6.9%)	0.00652	0.0899
Phototransduction - Homo sapiens (human)	KEGG	29	2 (6.9%)	0.00652	0.0899
Signal amplification	Reactome	31	2 (6.5%)	0.00742	0.0899
Visual phototransduction	Reactome	96	3 (3.1%)	0.00754	0.0899
Inactivation, recovery and regulation of the phototransduction cascade	Reactome	32	2 (6.2%)	0.0079	0.0899
The phototransduction cascade	Reactome	33	2 (6.1%)	0.00838	0.0899
mRNA 3,-end processing	Reactome	35	2 (5.7%)	0.0094	0.0899
Post-Elongation Processing of Intron-Containing pre-mRNA	Reactome	35	2 (5.7%)	0.0094	0.0899

2) Enriched gene ontology (GO) terms

67 genes (97.1%) from the input list are present in at least one GO category

gene ontology term		category, level	set size	candidates contained	p-value	q-value
GO:0019885	antigen processing and presentation of endogenous peptide antigen via MHC class I	BP 5	11	2 (18.2%)	0.00068	0.0936
GO:0001578	microtubule bundle formation	BP 5	67	3 (4.5%)	0.0018	0.123
GO:0019001	guanyl nucleotide binding	MF 5	394	6 (1.5%)	0.00276	0.0412
GO:0032550	purine ribonucleoside binding	MF 5	1828	14 (0.8%)	0.00458	0.0412
GO:0051297	centrosome organization	BP 5	97	3 (3.1%)	0.00512	0.234
GO:0007602	phototransduction	BP 5	115	3 (2.6%)	0.00819	0.26
GO:0042461	photoreceptor cell development	BP 5	41	2 (4.9%)	0.0095	0.26